Nanowire for Photonics

Li Na Quan[1,2†], Joohoon Kang[1,4,5,6†], Cun-Zheng Ning[7,8], Peidong Yang[1,2,3,4,*]

[1]Department of Chemistry, University of California, Berkeley, CA 94720, USA.

[2]Materials Sciences Division, Lawrence Berkeley National Laboratory, Berkeley, CA 94720, USA.

[3]Department of Materials Science and Engineering, University of California, Berkeley, CA 94720, USA.

[4]Kavli Energy NanoScience Institute, Berkeley, CA 94720, USA.

[5]Center for NanoMedicine, Institute for Basic Science (IBS), Seoul 03772, Korea

[6]Y-IBS Institute, Yonsei University, Seoul 03772, Korea

[7]Department of Electronic Engineering, Tsinghua University, Beijing 100084, China.

[8]School of Electrical, Computer and Energy Engineering, Arizona State University, Tempe, AZ 85287

[†]These authors contributed equally.

*Corresponding author. E-mail: p_yang@berkeley.edu (P.Y.)

Abstract: All photonic elements-based integrated circuits are a promising platform for device miniaturization beyond the limitation of Moore's law. Over the decades, one-dimensional (1D) nanowires have been focused for photonic circuitry because of their unique 1D structure to effectively generate and tightly confine optical signals as well as easily tunable optical properties. In this review, we categorize nanowires based on the optical properties (i.e., semiconducting, metallic, and dielectric nanowires) for their potential photonic applications (light emitter,

plasmonic and photonic waveguide). We further discuss the recent efforts of nanowire-based photonic elements integration towards next-generation optical information processors. However, there are still several challenges remaining before the nanowire is fully realized as photonic building blocks. The scientific and technical challenges and outlooks are provided to discuss the future directions.

CONTENTS

1. Introduction

One-dimensional (1D) nanowires are of great interest as a promising material platform for next-generation nanoelectronics and nanophotonic applications due to their unique electronic and optical properties. The properties are strongly correlated to their physically confined structures such as lengths, diameters, and chemical compositions. The structural characteristic (i.e., large aspect ratio) is beneficial to provide light propagating pathways towards photonic circuit integrations. Based on the chemical compositions, nanowires can be categorized into metallic, semiconducting and dielectric nanowires, where metallic and dielectric nanowires are suitable for plasmonic and photonic waveguiding applications, semiconducting nanowires are promising for light generation and sensing applications.[1]

Semiconducting nanowires are essential for optical signal generations based on their intrinsic bandgap-related optical transitions. Initially, the direct-bandgap nanowires such as II-VI and III-V compositions have been focused due to their efficient light emitting properties. Subsequently, nitride-based nanowires have been emerged because of their advantage in band gap tunability from the near infrared (indium nitride) to the near ultraviolet (gallium nitride) wavelength range. While these nanowires have been required harsh growth conditions, newly emerged halide-based perovskite nanowires are solution processable and exhibit remarkable structural and optical properties such as high emission/absorption efficiency, ionic bonding-based soft lattice, and defect tolerances. By exploiting the semiconducting nanowires, light emitting applications have been demonstrated. Especially, nanowires with well-faceted structures exhibit optical lasing as the structure plays a role for optical cavities to generate coherent light emission in nanoscale. The tunable wavelength of semiconducting nanowires provides a wide range of light emitting spectrum for light emitting diode applications. However, most of the light emitting

applications are currently demonstrated by optical pumping (*i.e.,* laser excitation). Lastly, the current efforts to demonstrate electrically-driven light generation are further discussed.

Metallic and dielectric nanowires are exploited as optical waveguiding applications. A waveguide is a key element for the photonic circuit integration to confine and propagate optical signals from transmitter to receiver. While light is confined in dielectric nanowires by total internal reflection, metallic nanowires propagate light with surface plasmonic polaritons. The dielectric nanowire diameter miniaturization for photonic waveguides is limited by the diffraction limit which is roughly half of the wavelength of the light in the waveguide. Although, this limitation can be overcome by utilizing metallic nanowires for plasmonic waveguides which confine light at the surfaces in a few nm, surface loss of plasmonic transmission with several orders of magnitude higher than that of photonic mode requires to balance the trade-off for the high-performance subwavelength optical waveguides. As one of the efforts, photonic-plasmonic hybrid waveguides have been demonstrated to take both advantages by optical coupling between metallic and dielectric nanowires.

Lastly, promising concepts for the realization of photonic elements-based integrated circuitry are discussed in the section 4. At the current stage, photonic circuit has been demonstrated as a prototype and required to be implemented in external circuits (e.g., field-effect transistors). We provide the challenges and outlooks towards high-performance photonic integrated circuit demonstrations.

2. Semiconducting Nanowires for Light Emitting Applications

Semiconducting nanowires have a fundamental absorption edge originated from the optical transitions of the intrinsic bandgap.[2] When electrons are excited to the upper band through optical excitation and leave unoccupied states in the valence band, an electron-hole pair is created due to the interband absorption process. The reverse process is called the interband emission where the excited electrons recombine with the unoccupied states in the lower band with emitting photons. The efficiency of interband transition is strongly dependent on the band structures. Based on the relative positions of the conduction band minimum and the valence band maximum in energy-momentum (E-k) diagram, the band gap can be a direct or indirect one. The conduction band minimum and valence band maximum appear at the same (or different) k in a direct (or indirect) band semiconductor. For indirect bandgap materials, the interband transition must involve a phonon to conserve momentum which results in much less transition efficiency and much longer radiative lifetime than direct bandgap materials. For example, since the excited electron and the hole are recombined at the same k vector in direct bandgap materials, no phonon-related thermal relaxation is involved, and thus the emitting efficiency is much higher.

2.1 Semiconducting nanowires for light generation and bandgap tunability

Direct bandgap semiconductors have the advantages for bandgap tunability using elemental, binary nanowires and alloy two or more materials with different bandgaps. Although the single crystalline epitaxial growth nanowire requires lattice matching in interfaces, the range of available bandgap is quite limited due to the less available choice of substrate and lattice mismatch in different components. Instead, by alloying different composition, all the bandgaps between certain constituent semiconductors can be achieved.

Alloying is a common technique for engineering the bandgap in semiconductor materials. The first examples of bandgap tunable III-IV compound nanowires on Si substrate was conducted by Samuelson group.[3] By modulating compositions in $GaAs_xP_{1-x}$ nanowire, the optical bandgap can be span from GaP (550 nm) to GaAs (900 nm). Compositional tunable $In_xGa_{1-x}P$[4] and $In_xGa_{1-x}N$[5] nanowires have also shown tunable emission from UV to near-infrared wavelength range (**Figure 1 a-b**). The temperature gradient approach was used to grow alloys within individual nanowires, such as CdSSe, ZnCdSSe (**Figure 1c**).[6-12] Such compositional tunability in single nanowire on the same chip could potentially realize the specific on-chip application such as laser. Light propagation happens asymmetric in compositionally graded nanowire, due to the propagation from higher energy emission to low energy bandgap regions.

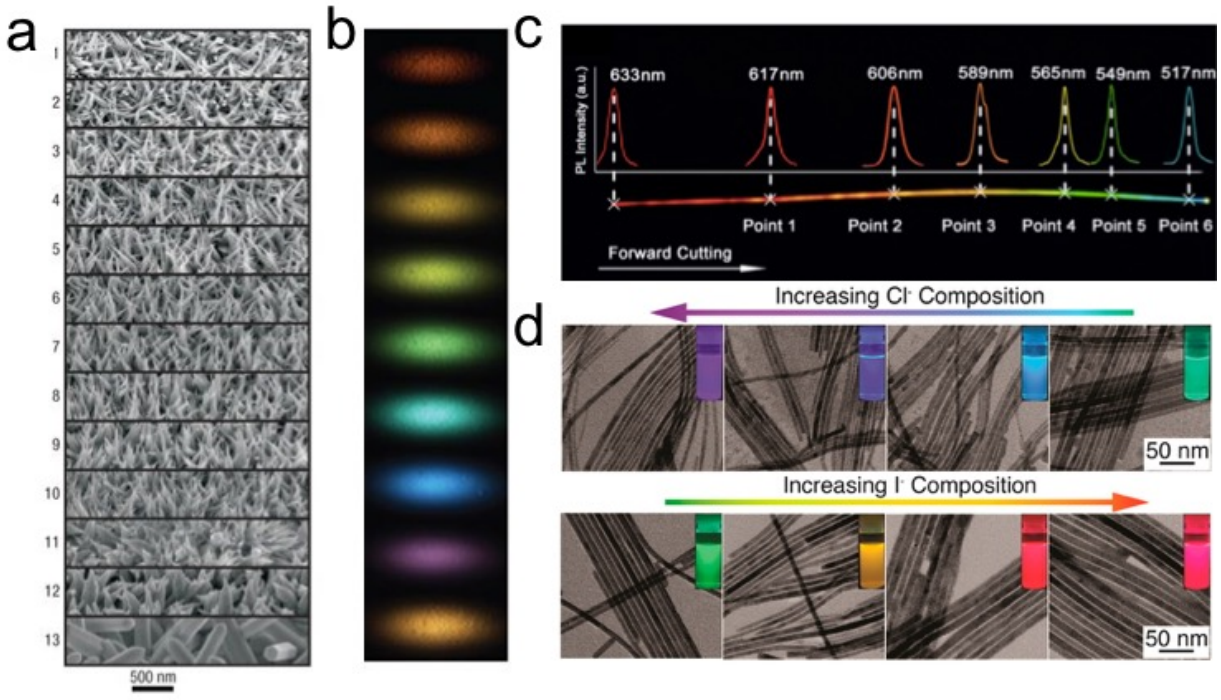

Figure 1. Bandgap tunable semiconducting nanowires. a) Scanning electron microscopy (SEM) images of $In_xGa_{1-x}N$ nanowire morphology and b) Color charge-coupled device (CCD) images of light emitting $In_xGa_{1-x}N$ nanowires. Adapted with permission from ref.[5]. Copyright 2007 Nature

Publishing Group. c) Localized PL spectra of bandgap graded CdSSe nanowires. Adapted with permission from ref.[7]. Copyright 2014 American Chemical Society. d) TEM images of $CsPbX_3$ nanowires different halide composition. The insets show the evolution of the UV-excited emission colors upon the formation of mixed-halide alloy nanowires. Adapted with permission from ref.[13]. Copyright 2016 American Chemical Society.

Yang and co-workers have firstly demonstrated colloidally synthesized halide perovskite nanowires in solution phase without any catalyst, at room temperature (**Figure 1d**).[13,14] Their ionic-bonding characteristics offer soft crystal lattice and allow rapid ionic dynamics at solid-liquid-vapor interfaces. Halide perovskite nanowires such as $CsPbBr_3$ and $CsPbI_3$ nanowires exhibit a direct bandgap nature and strong luminescence properties. Tunable wavelength (blue to near IR) resulting in multi-color nanowire heterojunctions has been demonstrated using $CsPbX_3$ (X = Cl, Br and I) with the combination of mixed halide composition.[15]

Nanowire for photonic applications initiated by developing nanoscale wavelength tunable lasers, which lead to white light generation,[16] photonic integrated circuit[17,18] and sensing applications. "Laser" is the abbreviation of "Light Amplification by Stimulated Emission of Radiation". As it stands for, laser is based on the quantum-mechanical process of stimulated emission.[19] Unlike spontaneous emission, the process of stimulated emission results in optical amplification. A laser cavity formed naturally in a nanowire gain medium with reflectors at either ends.[20] The semiconductor nanowire is a promising material platform for use in the next generation of laser applications due to the capability of emission wavelength tuning, complementary metal–oxide–semiconductor (CMOS) integration, and miniaturization.[21-25] Furthermore, a well-faceted

nanowire with high refractive index plays a role simultaneously not only as an optical gain medium, but also an optical cavity structure.

The first demonstration is ultraviolet nanolaser at room-temperature using ZnO nanowires array in 2001 (**Figure 2 a-c**).[26] The bottom-up growth approach allows the formation of a well-faceted ZnO nanowire structure which leads to the formation of optical cavity. However, the structural polydispersity of each ZnO nanowire in an array, such as variations of diameter from 20 to 150 nm and lengths from 2 to 10 μm, gives an average signal of the resulting spectra from individual nanowires. To further verify the nanowire structure acting as a Fabry-Pérot cavity, the emission spectra were obtained from an individual nanowire which shows lasing peaks and much stronger intensity from the end facets than the side surfaces. This concludes that the lasing process requires a minimum diameter for sufficient waveguide confinement.[20]

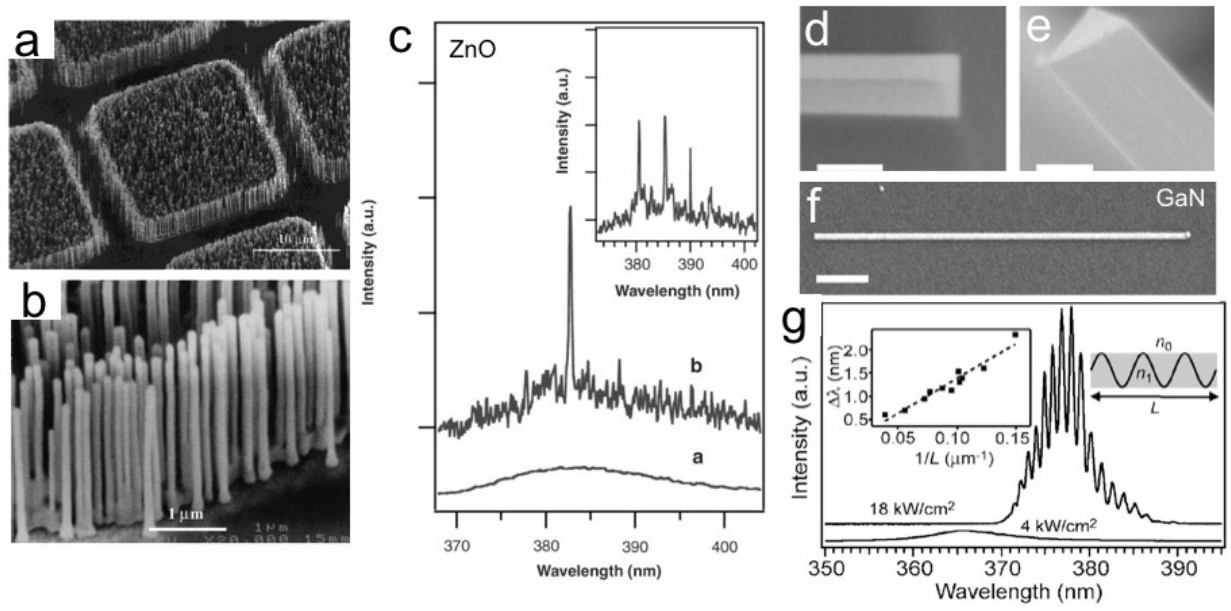

Figure 2. Semiconducting nanowire lasers. a, b) SEM images of ZnO nanowire arrays grown on sapphire substrates for the first nanowire laser demonstration. Adapted with permission from ref. [27]. Copyright 2001 AAAS. Adapted with permission from ref.[30]. Copyright 2001 American

Chemical Society. c) Light emission spectra of ZnO nanowire arrays at above (inset b) and below (inset a) the lasing threshold. Adapted with permission from ref. [27]. Copyright 2001 AAAS. d-f) SEM images of GaN nanowires with triangular cross section and g) Light emission spectra of single GaN nanowire, which Fabry–Pérot cavity mode lasing. Adapted with permission from ref. [28,29]. Copyright 2005 American Physical Society.

After the first demonstration of ZnO nanowire-based nanolasers, other semiconductor nanowire-based lasers were soon demonstrated including GaN (**Figure 2 d-g**),[28,30-32] InGaN,[33] CdS,[34] CdSe,[35,36] CdSSe,[8] GaAs,[37] InGaAs,[38] AlGaAs,[39] ZnS,[40] GaSb,[41] and InP.[42] Furthermore, ultraviolet lasing from an epitaxially-grown AlGaN/GaN core/shell heterostructure was demonstrated.[43] Tailoring the emission wavelengths was only achieved for a limited wavelength range in these studies and also impractical to generalize in some cases. The emission wavelengths can be tuned by tailoring structures or tuning the dielectric environment of the cavity. But the most efficient method of wavelength engineering is the tuning of the bandgap of the emitting materials through alloy composition control.[8,10,12,16,44] Optical properties of semiconductor and dielectric nanowires are listed in **Table 1**.

	Nanowire composition	Bandgap (eV)	Refractive index (visible-NIR)	Ref.
Semiconductor	Al_xGa_yAs	1.8	1.4	[45,46]
	GaAs-$Ga_xIn_{1-x}P$	1.6- 1.4	3.6	[47]
	CdS	2.4	2.1	[34]
	GaSb	0.8	3.8	[41]
	CdS_xSe_{1-x}	2.4-1.7	2.7-1.7	[8,12,48]
	GaAs/GaAsP	1.5	3.7-3.6	[49]
	$Zn_xCd_{1-x}S_ySe_{1-y}$	-	3.4-1.7	[9,10]
	InGaAs/GaAs	1.3	3.7	[50-52]
	InP	1.3	4.4-3.1	[53]
	$MAPbX_3$ (X=I, Br, Cl)	3.2-1.6	2.3	[54,55]
	$FAPbX_3$ (X=I, Br, Cl)	2.2-1.5	2.5	[56]
	$CsPbX_3$ (X=I, Br, Cl)	3.0-1.7	-	[14,57]
Dielectric	TiO_2	3.2	3.3-2.7	[58]
	SnO_2	3.6	2.1-2.0	[59]
	ZnS	3.7	2.6-2.3	[60]
	$Al_xGa_{1-x}N$	5.3	2.3	[43]
	GaN	3.4	2.5	[24,28,30]
	ZnO	3.4	2.0	[27,61,62]

Table 1. Optical properties of semiconductor and dielectric nanowires.

Rational design of nanowires leads to the structure complexity which enables functional electronic and photonic capabilities. Multi-quantum well core-shell structured nanowires $(InGaN/GaN)_n$ yielded lasing in a broad range of wavelengths from 365 to 494 nm (**Figure 3 a, b**).[33] Such tunable nanoscale gain medium that coupled to the optical cavity is essential for developing miniaturized lasers. A single-mode lasing has been discovered based on the formation of a cleaved-coupled cavity, contains two Fabry–Pérot cavities coupled to an air gap.[31] By cleaving a nanowire with the controlled gap position and the size, the device enables to control the lasing threshold of all the longitudinal modes.[31] This cleaved-coupled cavity structure was demonstrated based on a GaN and shown lower lasing threshold than the single component nanowires (**Figure 3 c, d**). Furthermore, nanomanipulation in nanowires have realized by modulating the structures from line shape to pseudoring conformation.[24,63] Light emission wavelength, lasing Q factors can

be manipulated in nanoring laser, compared to linear shape, due to the side-by-side coupling of nanowire ends.

As mentioned early on, such control can be most efficiently realized through the growth of alloy nanowires. Tunable lasing from a single substrate was realized by spatial grading of alloy composition from CdSe to CdS, allowing the lasing wavelength to be tuned between 700 nm to 500 nm (**Figure 3e**).[8,48] Simultaneous red[64] and green lasing was also achieved in a single nanowire with dynamically tunable colors continuously from red to green.[12] More interestingly, color tunable lasing was demonstrated[16] in the full visible spectrum by simultaneous lasing in red, green and blue from a single semiconductor nanosheet structure, allowing lasing in white from a single monolithic piece of semiconductor for the first time.[16] Wide wavelength tunable nanowire laser can also be possible based on the absorption-emission-absorption process by changing the length of nanowires.[65] Such full-color lasers or white lasers could find many potential applications in laser lighting, laser illumination, and laser displays, especially with the recent increased interests in various micro displays.

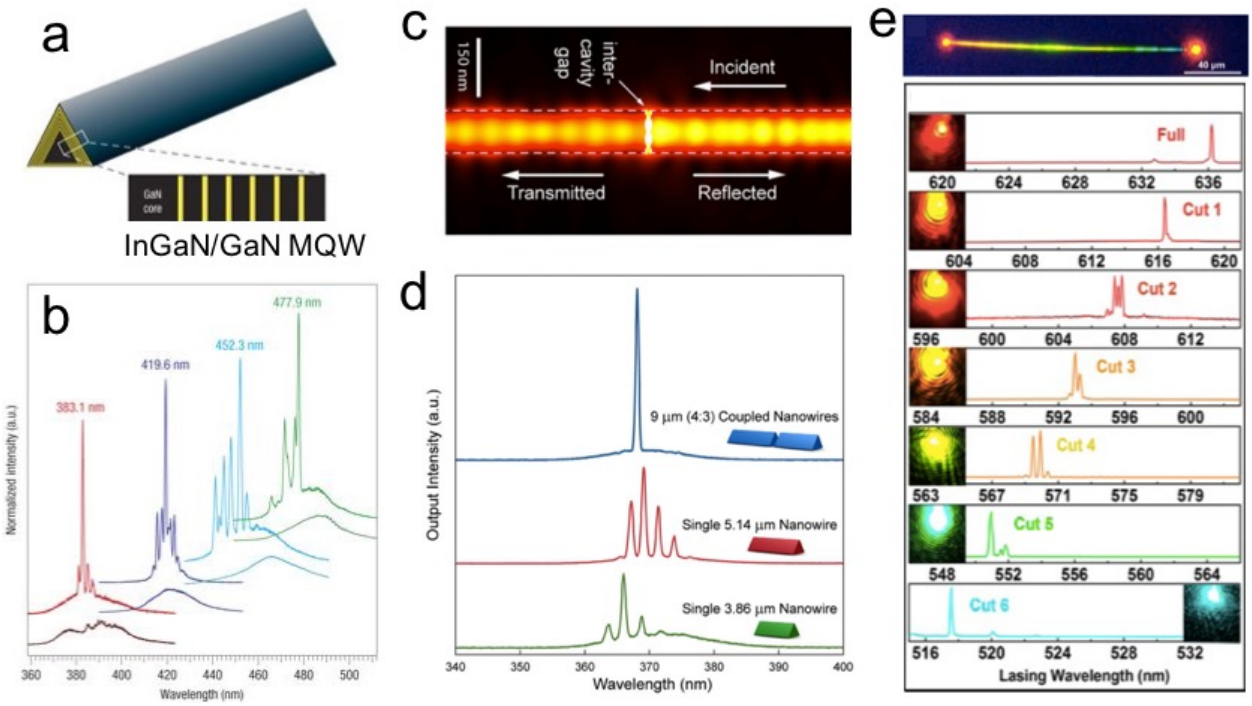

Figure 3. Rational design of semiconducting nanowires for lasing. a) Multi-quantum well nanowire structure with InGaN/GaN compositions and b) Light emission spectra of 26 multi-quantum well InGaN/GaN nanowire at above lasing threshold. Adapted with permission from ref. [33]. Copyright 2008 Nature Publishing Group. c) Simulated electrical field of cleaved coupled nanowire and d) Single wavelength lasing from the coupled cavity structure (blue) as opposed to the gapless nanowires lasing (red and green). Adapted with permission from ref.[31]. Copyright 2013 National Academy of Sciences. e) Optical microscope images of nanowires with high excitation power density at above lasing threshold and corresponding spectra of nanowires from full to cut. Adapted with permission from ref.[7]. Copyright 2014 American Chemical Society.

Beyond the conventional II-V and III-V semiconductor compounds, ABX_3 structured halide perovskites have recently emerged as a promising material platform for applications due to the unique light-matter interacting properties such as high absorption or emission efficiency, long

diffusion length, and low trap density (**Figure 4**).[14,22,66-72] In addition to the remarkable optical properties of halide perovskites, it is even more advantageous to synthesis such materials under ambient condition in contrast to the II-V and III-V semiconductor compounds relying on high temperature or high-vacuum process. Furthermore, the soft nature of the halide perovskite crystal lattice provides flexible wavelength selection by a simple anion-exchange process.[66]

Lasing in a perovskite nanowire was firstly demonstrated using an organic-inorganic hybrid nanowire, methyl ammonium lead halide ($MAPbX_3$). Single-crystalline halide perovskite nanowires were synthesized from a $PbAc_2$ (lead acetate) thin-film immersed in a methyl ammonium halide precursor solution in the ambient conditions. The perovskite nanowires show lasing behavior at room temperature and further the emission wavelengths are tunable based on the composition ratio of the halide precursors across the visible spectrum.[66] This first demonstration of the halide perovskite nanowire-based lasing achieves both high-quality optical materials synthesis under the ambient conditions and a broad range of tunable emission wavelengths by simply changing the ratio of halide salts. Furthermore, this solution-based simple synthesis approach allows to have a large scale $MAPbX_3$ nanowire arrays using a polydimethylsiloxane rectangular groove template.[67,68] Specifically, precursors dissolved in polar solvent was confined in the polymer template and form a $MAPbX_3$ nanowire arrays with well-controlled dimensions and uniform geometries. The arrays lase at 770 nm with a good photostability exceeding 4×10^7 laser pulses.[67] Although the hybrid $MAPbX_3$ perovskite nanowires show excellent lasing performance, a critical limitation of their ambient instability motivates to replace the reactive methyl ammonium cation with an alternative cation. In efforts to replace the reactive methyl ammonium cation to an alternative cation, formamidinium (FA) has been utilized for the halide perovskite nanowire formation.[73] In a recent report, $FAPbX_3$ nanowires

were synthesized similar to the $MAPbX_3$ nanowires formation, a $PbAc_2$ thin-film immersed in a FA halide precursor solution in the ambient conditions. As-synthesized $FAPbX_3$ nanowires exhibit an excellent tunable-wavelength lasing performance over 10^8 excitation cycles at room temperature with remarkably improved ambient stability.[72]

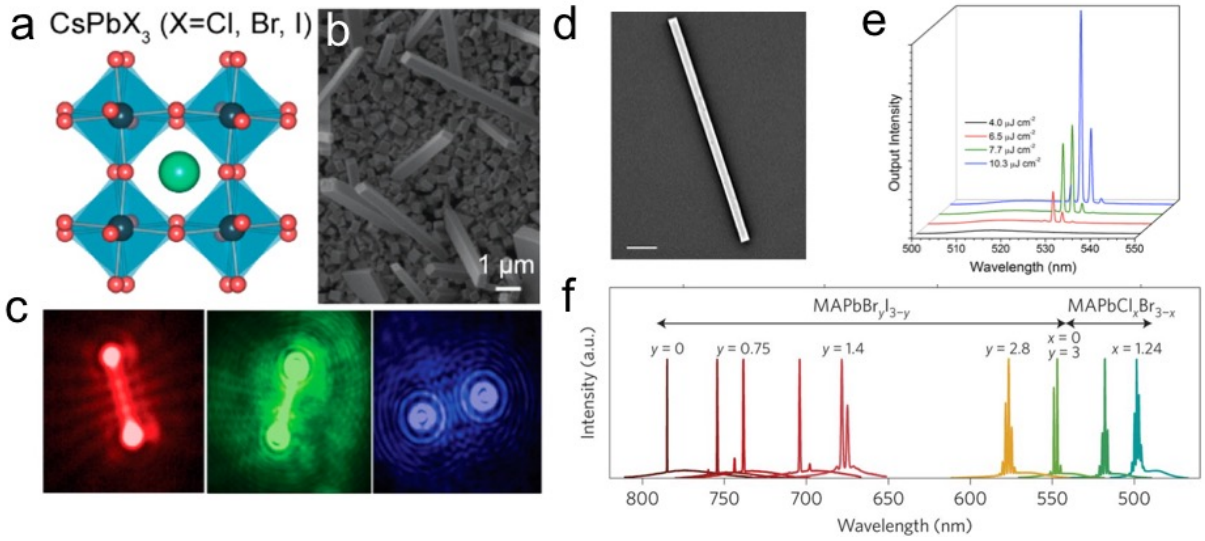

Figure 4. Halide perovskite single nanowires for lasing. a) Crystal structure of ABX_3 metal halide perovskites, b) SEM image of as grown multiple $CsPbBr_3$ perovskite nanowires on the substrate and c) Optical images of nanowires under high excitation pump power at above lasing threshold, with different wavelength from red to blue. Adapted with permission from ref.[57]. Copyright 2016 American Chemical Society. d) Isolated single $CsPbBr_3$ nanowire and e) Power dependent light emission spectra of $CsPbBr_3$ single nanowire at above lasing threshold. Adapted with permission from ref.[14]. Copyright 2016 National Academy of Sciences. f) Wavelength tunable lasing at room temperature from single crystal perovskite nanowires. Adapted with permission from ref.[55]. Copyright 2015 Nature Publishing Group.

Alternatively, Cs-based all-inorganic halide perovskites have emerged to replace the organic components (MA or BA) by Cs for further improved chemical stability. The first study has shown the improved environmental stability by incorporating Cs ions partially into the FA-site.[73] And this stability improved halide perovskite has been utilized for solar cell demonstration with enhanced stability under continuous light illumination.[73] The first demonstration of the stability improved Cs-based all-inorganic halide perovskites accelerates the synthesis of Cs-based 1D perovskite nanowires as a new pathway towards high emission efficiency and ambient stability.[13,74-76] Followed by the Cs-based nanocrystals formation by a colloidal synthesis approach,[13,74-76] Cs-based perovskite nanowires have also been synthesized via non-colloidal[14] and chemical vapor transport (CVT) method.[77,78] The non-colloidal $CsPbBr_3$ nanowires further exhibited lasing at low thresholds and relatively high Q-factors in comparison with the hybrid perovskite nanowire lasers. Furthermore, the all-inorganic perovskite nanowires were much more stable under lasing conditions (e.g., stable even after 10^9 excitation cycles).[14] The all-inorganic perovskite nanowires which require mild synthesis conditions, exhibit stability and high lasing performance can be a promising material platform for the applications of a nanowire-based lasers for the future.[68]

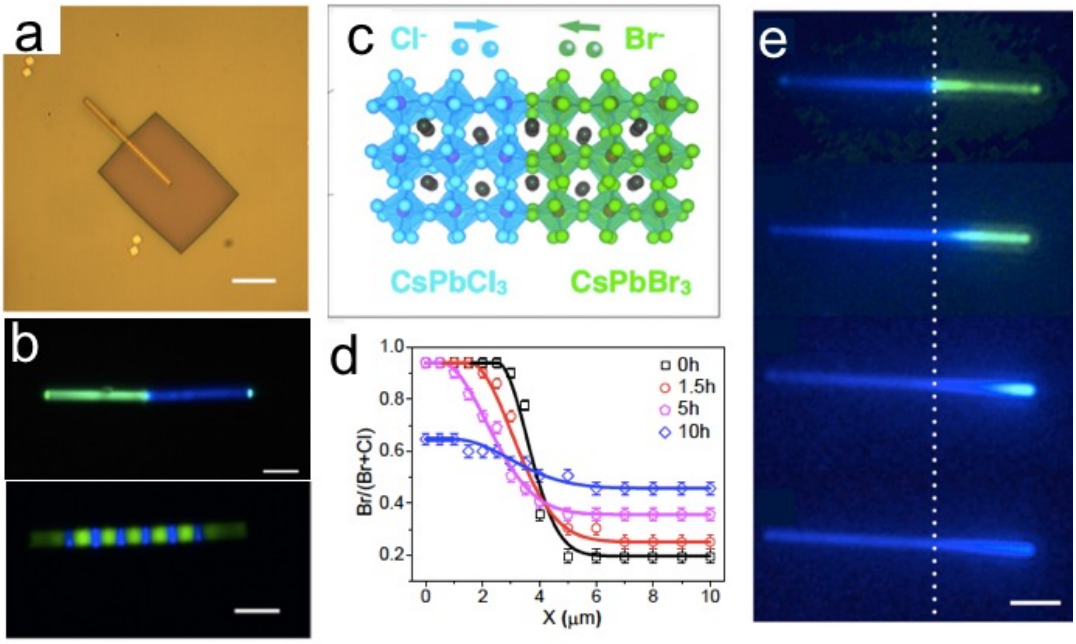

Figure 5. Unique property of heterojunction in perovskite nanowires. a) Optical microscope image of $CsPbBr_3$ nanowire coated with polymer and open a portion using the electron beam lithography, and b) under photo excitation. Adapted with permission from ref.[15]. Copyright 2017 National Academy of Sciences. (c-e) Evolusion of Cl/Br anion diffusions at high temperature (100 °C) along the $CsPbCl_3$–$CsPbBr_3$ nanowire, and corresponding PL images. Adapted with permission from ref.[79]. Copyright 2018 National Academy of Sciences.

As the lead halide perovskites show predominant ionic bonding character, results in highly dynamic crystal lattices, inherently allowing rapid ion exchange at solid-vapor and solid-liquid interfaces. These reactions afford a high degree of ion diffusion, which plays a major role in optoelectronic performance. As such, a microscopic study of both the kinetics and thermodynamics of ion exchange and diffusivity has been carried out.[15,79] Multi-colored $CsPbX_3$ perovskite nanowire heterojunctions have been fabricated using electron-beam lithography technics with tunable PL emission wavelength from UV to near IR (**Figure 5**).[34] Ionic exchange

reactions in perovskites was studied firstly using nanofabrication techniques and multiscale theoretical modeling to investigate halide anion inter-diffusion in $CsPbBr_3$–$CsPbCl_3$ single crystalline nanowire heterojunctions.[83] Wide-field and confocal photoluminescence measurements enabled the direct observation of intrinsic lattice diffusivities, which were found to be several orders of magnitude lower than those reported for polycrystalline thin films. Molecular simulations determined low energetic barriers for halide vacancy formation as well as vacancy hopping, highlighting the role of the soft ionic lattice in facilitating anion exchange and diffusion. These findings provide an important foundation for the fabrication of novel heterostructures. Furthermore, PL emission intensity of $CsPbBr_3$ nanowires have been significantly improved by oxygen gas exposure by passivating of the excess lead dangling bonds with oxygen molecules.[80] This passivation scheme results in the 4-fold increase of radiative recombination lifetime by effectively reducing the non-radiative recombination channel on the deep level trap states of perovskite surface.

2.2 Electrically-driven light emission

Above mentioned semiconductor nanowires are ideally suited for electrically driven lasers and light emitting diode devices. A single nanowire provides both a high quality gain material and an ideal waveguide to confine optical waves[20]. The simultaneous confinement of electron-holes and photonics in the same physical entity assures the efficient interactions of electrons and photons. The insensitivity of nanowire growth to the substrate materials allows semiconductor alloys of different compositions to be grown on the single platform or within a single monolithic piece of semiconductor, making it possible to have mutli-color emission or lasing for full color electrically driven applications[8,10,12,22,44]. Photoluminescence (PL) property has been investigated for many

types of nanowires such as ZnO,[81] GaN,[82] InGaN,[5] and GaP/GaAs.[83] ZnO is a large band-gap (3.35 eV) semiconductor at room temperature, with fascinating properties for ultraviolet LEDs and lasers.[84-89] The integration of traditional direct bandgap II-IV and III-V nanowires with Si nanowires enables to produce multicolored, electrically driven nanoelectronics-photonic systems[90].

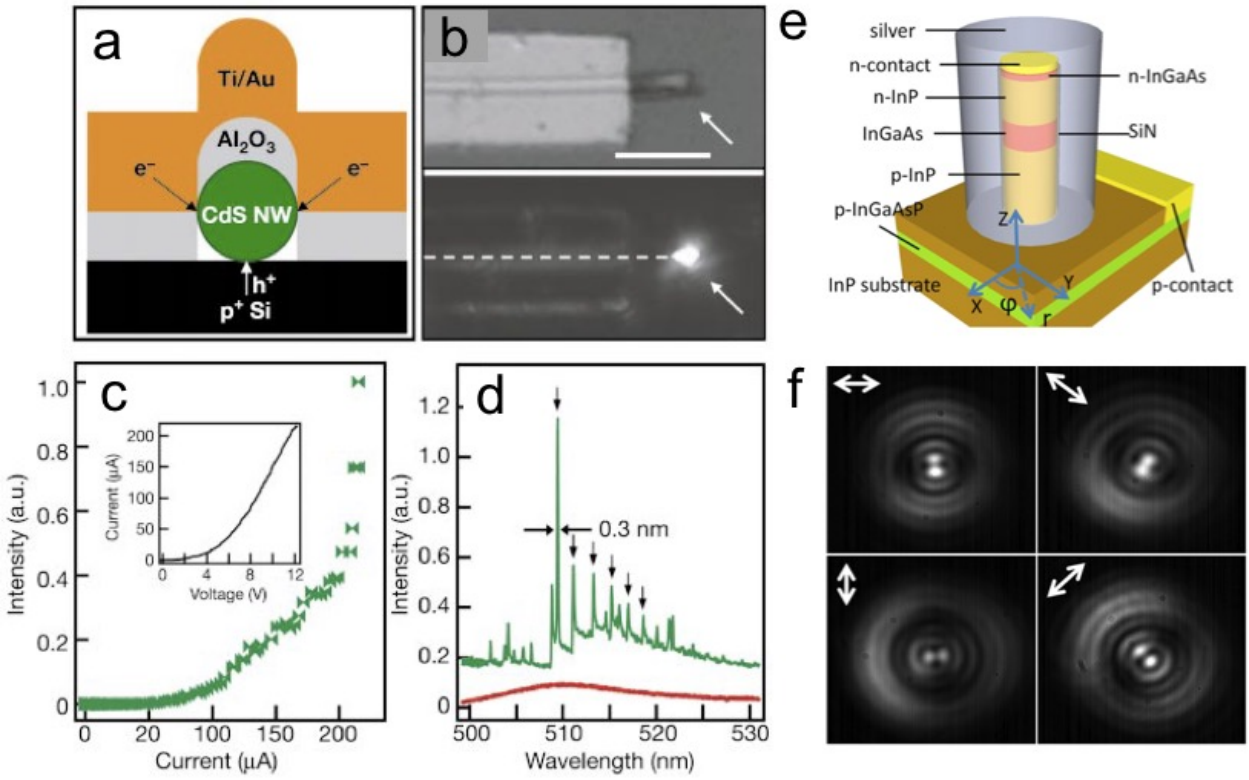

Figure 6. Electrically driven nanowire lasers. a) Cross section diagram of nanowire laser device, b) Optical image of CdS nanowire laser device under the operation, the arrow highlights the end of CdS nanowire, where emit the light, c) Light emission intensity increases as increase the inject current into device and d) Electroluminescence spectra of nanowire device, the arrows highlights laser cavity modes with a narrow spacing. Adapted with permission from ref.[91]. Copyright 2003 Nature Publishing Group. e) Metallic cavity lase structure with circular shape cross section and f) Optical images of laser output using near IR camera. Adapted with permission from ref.[29,92]. Copyright 2013 American Physical Society.

Electrically driven lasers can be used in wide range of technologies including information storage and medical therapeutics.[93] Most of the electrical injection in semiconductor laser relies on metal cavity, which serves as electrode in photonic crystal laser.[94-96] However, lasing from electrical injection in single nanowire level device is sufficiently different from the bulk semiconductor devices, requires unique electrical injection configurations.[97] One of the first electrical driven semiconductor nanowire laser was developed from Lieber group (**Figure 6 a-d**).[91] Such electrical injection nanolaser device is configured with *n*-type semiconductor nanowire assembled onto *p*-type electrodes. In this case the holes are injected through the nanowire cavity and strong light emission from the ends of the nanowires. Later on, Ning and co-workers studied electrical injection in *p-n* junction core-shell nanowires and *p-i-n* longitudinal nanowires using numerical simulation[97]. The longitudinal structure requires higher bias and doping concentration, compare to the core-shell nanowires in electrical driven devices. Same group has also developed electrically driven metallic cavity nanolasers, based on the structure with InP/InGaAs/InP nano-pillar and SiN layer was coated on its sidewall (**Figure 6 e, f**).[92]These metallic cavity nanolaser can be used as azimuathally polarized beam, driven by electrical injection.

ZnO nanowires has been shown strong excitonic PL emission at a wavelength of 384 nm, along with a broad luminescence from defects at room temperature around 600 nm wavelength. Electrically-driven luminescence properties been explored from ZnO/polymer hybrid interface, due to a strong defect induced emission in air (**Figure 7**).[81,85] Many research groups realized electroluminescence (EL) by using *p* or *n*-type ZnO nanowires based on homojunctions.[98,99] The *n*-type ZnO nanowires were epitaxially grown on *p*-type GaN thin film to generate heterojunctions and used to fabricate LEDs.[86,87] The band to band and defect transitions between the ZnO

nanowires and the *p*-GaN thin film is a key factor to achieve EL at room temperature resulting in the stable light emission with a low turn on voltage. These ZnO nanowire arrays fabricated on GaN substrate used solution phase synthesis method, and each of the single nanowire serves as a light emitter.[89] The *p*-*n* junction LEDs have shown the external quantum efficiency (EQE) of 2.5 %. Another example of using *p*-*n* homojunction of the ZnO nanowire is doping phosphorus (P) as a *p*-type ZnO to produce *p*-doped segments *n*-type ZnO nanowire. The cathodoluminescence (CL) emission was observed at the emission wavelength of 340 nm due to the high electron carrier concentration.[100] Vertically oriented ZnO nanowires that embedded in polymeric matrix have been used to fabricate the flexible LEDs, which is potentially important for stretchable optical device applications.[101]

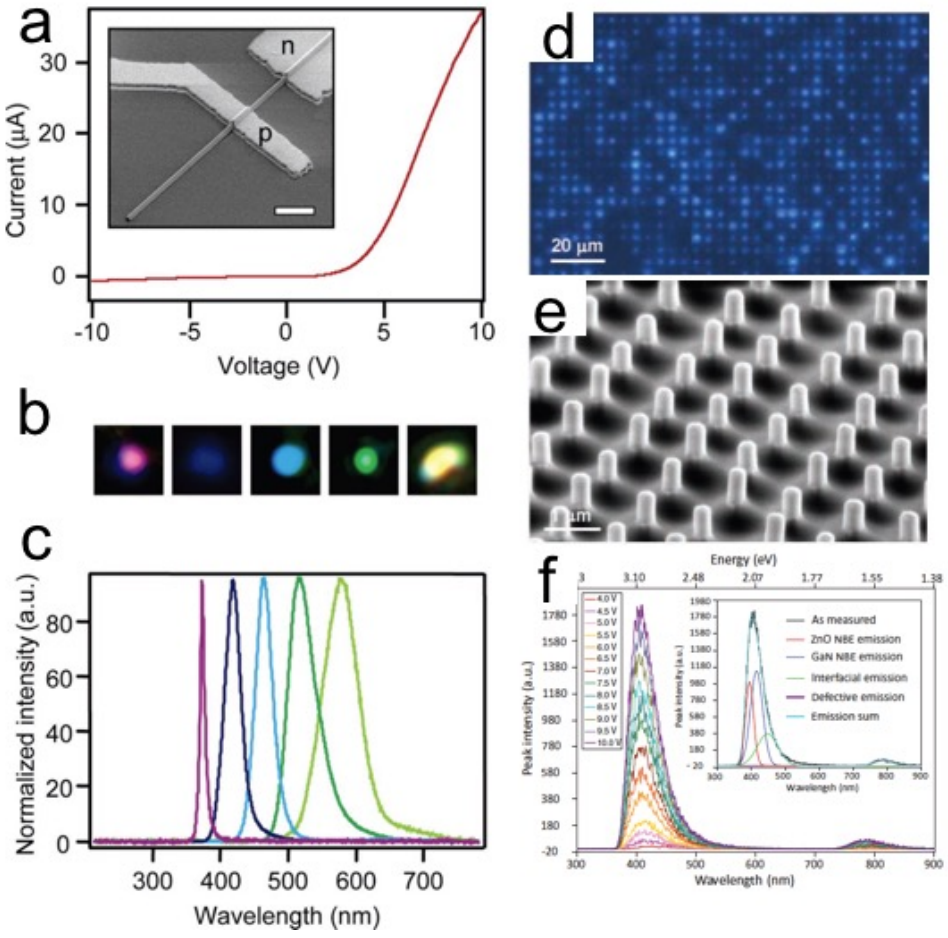

Figure 7. Semiconductor nanowire for light emitting diodes. a) Core-multi-shell nanowire device performance with current-voltage measurement and SEM image of the LED device (inset), b) Optical microscopy images from core-multi-shell nanowire LEDs and c) Electroluminescence spectra from core-multi-shell nanowire device. Adapted with permission from ref.[102]. Copyright 2005 American Chemical Society. d) The optical image with LED device working, e) SEM image of SiO_2 coated ZnO nanowires and followed by wrapping polymer and f) Electroluminescence spectra of LED device under different voltage. Adapted with permission from ref.[89]. Copyright 2010 John Wiley and Sons.

The compositional tunability in III-V semiconductor $In_xGa_{1-x}N$ nanowires allows tunable PL emission from UV to near infrared wavelengths.[5] The core-shell structured nanowires with the composition of *p*-type AlGaN with GaN nanowires has enabled to produce tunable EL emission from 365 to 600 nm with high device performance.[102] Indium phosphine (InP) nanowires with controlled doping level have also been used to fabricate the nanoscale LEDs and their direct bandgap nature offers *p*-*n* junctions as a basis of optoelectronics.[103] Self-aligned quantum dot at the end of the *n*-InP and *p*-InP nanowires offers these materials as promising candidates for electrically pumped quantum optics application.[104] Using semiconductor organic-inorganic halide perovskite nanowire arrays, Yang and co-workers has successfully integrated $MAPbBr_3$ nanowires into LED applications.[105] The interconversion of halide components in hybrid perovskites revealed by using the post-synthetic methods to further control the EL emission wavelengths.

3. Dielectric and Metallic Nanowires for Optical Waveguides

Towards all-photonic integrated circuit realization, optical waveguide is one of the essential elements to route optical information between optical transmitter and receiver. Over the several decades, Si has been focused, inspired from a conventional Si-based integration circuit, and utilized for optical gain,[106] modulators,[107] lasing,[108] and nonlinear optics.[109] However, Si has an indirect bandgap in an infrared range which makes it difficult to realize efficient photonic elements in the visible/UV spectral regions. Alternatively, 1D nanowire has versatile advantages for photonic applications such as size and composition tunability, various optical properties, low surface roughness (especially, for chemically-grown nanowires), and capabilities to operate both above and below the diffraction limit.[110] Especially, a large aspect ratio provides a promising material platform for optical waveguide or fiber applications because the diameter is compatible to the characteristic length scale of various fundamental phenomena and the length is sufficient to connect each optical element. Based on light confinement mechanisms, the nanowire-based waveguides are mainly categorized into photonic and plasmonic waveguides. While the photonic waveguides route optical energy through nanowire inside, the plasmonic waveguides happen close to nanowire surface. As the routing mechanism is totally different, each waveguide shows completely distinct optical performances. Although there are remarkable advances in both areas, a common major technical challenge for the nanowire-based waveguides is to achieve a device miniaturization by overcoming the light diffraction limit.

Dielectric nanowires such as a conventional SiO_2 nanowire and subsequent binary oxides nanowires have been exploited for a photonic waveguide which relies on electromagnetic response of bound electrons. In a photonic waveguide, as shown in Figure 8a, photons propagate by

diffraction or total internal reflection in a dielectric nanowire and the diameter of nanowire is limited by the Abbe diffraction limit (~ half of the photon wavelength in the nanowire)[111]:

$$d = \frac{\lambda}{2n \sin \theta}$$

where d, λ, and n are diffraction limit, wavelength of light in the material, and refractive index of the material, respectively. To miniaturize a photonic waveguide below the subwavelength region, high refractive index single crystalline nanowires have been utilized. For example, SnO_2 nanowire (n = 2.1) has been demonstrated for the subwavelength photonic waveguide with low propagation loss (1 – 8 dB/mm) at visible frequencies.[59] However, further miniaturization is still limited by the diffraction limit. To overcome this limitation, surface plasmonic polaritons (SPPs) based plasmonic waveguide modes have been emerged to study collective oscillations of quasi-free charges on metal nanowires. Surface plasmons have two different types, localized surface plasmons (LSPs) and propagating surface plasmon polaritons (SPPs). For the surface plasmonic waveguide mode, SPPs will be only considered in this section. Since the SPPs energy is tightly bound at metal nanowire surfaces in few nanometer-scale (Figure 8b), the plasmonic waveguide mode can be considered for deep subwavelength optical waveguide demonstrations.[111] Electric field distributions in the dielectric SnO_2 and the metallic Ag nanowire are indicated in Figure 8c, which shows that the optical propagation pathways in the nanowire or on the nanowire surface for photonic and plasmonic waveguide, respectively. Although the electric field of plasmonic waveguide mode (below panels in Figure 8c) is tightly concentrated on the nanowire surface which is good for the device miniaturization, the optical propagation losses in metal nanowires are several orders of magnitude larger than those in dielectric nanowires due to defects formation on the metal surface under ambient conditions. For example, the propagation loss of Ag nanowire-based waveguide is close to 1 db/μm^3.[111]

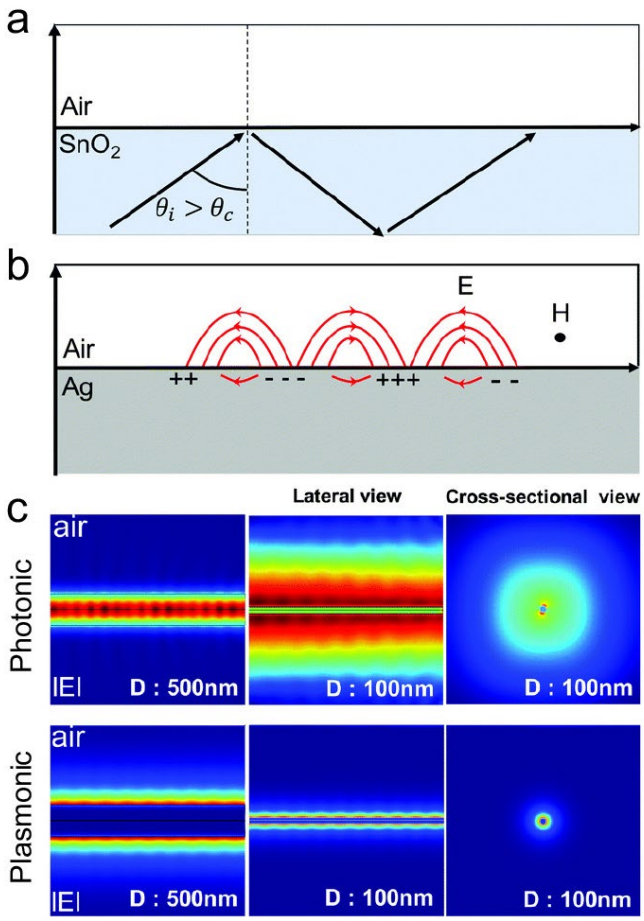

Figure 8. Light propagation mechanisms in dielectric nanowire via total internal reflection (a) and in metallic nanowire via SPPs (b). (c) Electric field distribution in photonic and plasmonic nanowire waveguides with 500 and 100 nm diameters. Adapted with permission from ref.[111]. Copyright 2018 Royal Society of Chemistry.

3.1 Dielectric nanowires for photonic waveguides

Light propagates in a photonic waveguide by diffraction or total internal reflection. In a structure that a dielectric nanowire with high refractive index (n_1) is encapsulated with a low refractive index (n_2) dielectric cladding or air, photons are propagating via total internal reflection at the interface when the incident angle is larger than the critical angle which equals to $\sin^{-1}(n_2/n_1)$.[111] While the incident photons with the angles larger than the critical angle are captured

and modulated in the waveguide, other photons entered with the smaller angles leak out from the waveguide.

For the photonic device miniaturization, it is limited to confine light with a wavelength much larger than the diameter of dielectric nanowire. As discussed earlier, the smallest diameter is proportional to $\lambda/(2n)$. For deep subwavelength waveguide, dielectric nanowires with large refractive indices have been explored by replacing SiO_2 (n = 1.5). For example, a wide bandgap (3.6 eV) SnO_2 nanoribbon (n = 2.1) has been demonstrated as an excellent subwavelength waveguide (Figure 9a-b).[59] Figure 9b is a photoluminescence image of the waveguiding nanoribbon under laser excitation. Furthermore, the SnO_2 nanoribbons can be optically coupled with active nanowires (GaN and ZnO) through tangential evanescent coupling where the active and passive materials interact over a few microns, which can be a direction to demonstrate more functional geometries like Mach-Zehnder interferometers. Subsequently, four nanoribbons were assembled into a rectangular grid to test inter-cavity optical coupling (Figure 9c).[112] As shown in Figure 9d, direct laser excitation from one nanoribbon end triggered emission from all seven ends, with the relative intensity: $1 >> 6 > 4 \sim 7 > 3 > 5 > 2$. The intensity order is coming directly related to the number of junctions through the optical pathways.[112] This grid-like nanoribbon integration shows a capability of guiding light for a photonic logic circuit demonstration.

In addition to the guidance of light, one crucial challenge for photonic nanowire-based subwavelength optics is to demonstrate a tunable source of coherent radiation. Nonlinear optical processes originated from high optical intensities and long interaction lengths can be a key to tune the frequency of light via second harmonic generation (SHG) and sum frequency generation (SFG).[113] While bulk materials result in low efficiency due to a reduced confocal parameter induced interaction length shortening, 1D photonic waveguiding nanowires enable high optical

intensities. For several years, a silicon-on-insulator (SOI) nanowire structure has been focused due to its high refractive index for tight light confinement.[109] Subsequently, a perovskite oxide KNbO3 nanowire has been reported for nonlinear optical probes because of its large effective nonlinear optical coefficients and large refractive indices (n = 2.1 – 2.5).[113] Figure 9e shows a schematic of laser trapped a single KNbO3 nanowire in closed aqueous chambers with a trap wavelength at 1064 nm and the radiation profile as a function of position along the nanowire's long axis by changing the focus. The emitting wavelength at the end of the KNbO3 nanowire is 531 nm (Figure 9f), which corresponds to the SHG signal of the 1064 nm trapping wavelength.[113] As a control experiment, Si nanowire (black line) did not produce light emission, as another evidence of the green emission from the KNbO3 nanowire induced SHG. Furthermore, tunable emission wavelengths have been obtained from a single KNbO3 nanowire at 423 and 454 nm (SFG modes) and 525 and 700 nm (SHG modes) by introducing different frequencies of femtosecond lasers.[113]

Unlike the light trapped in photonic nanowires, evanescence fields (i.e., light travelling outside of the waveguide) can be a promising platform for optical sensors which require high sensitivity to the external environment. As one example, a photonic nanowire based single cell endoscopy has been reported, which demonstrates light in and out of a single living cell without cell damage (Figure 9g).[114] The nanowire endoscope, consisted of a nanowire waveguide and a tapered optical fiber, can be inserted into a single living cell and deliver quantum dots in the cell membrane (inset, Figure 9g).[114] This approach is a promising candidate for high-resolution optical sensing, imaging, and spatiotemporally precise drug delivery systems.

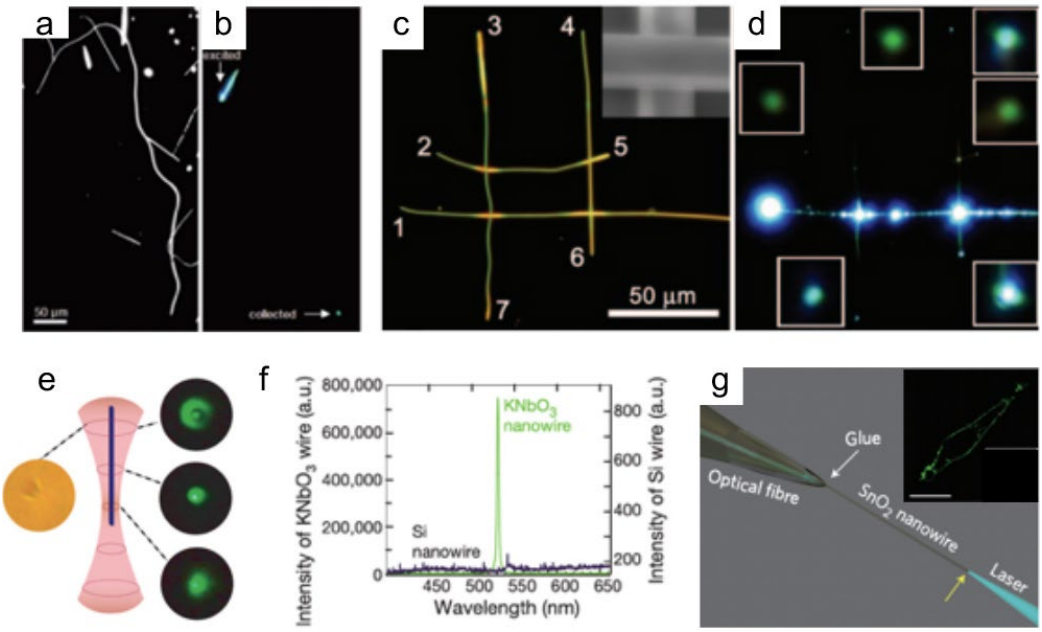

Figure 9. Applications of photonic nanowire waveguides. (a) Optical waveguiding in a SnO2 nanoribbon. (b) PL image of the waveguiding nanoribbon under laser excitation. Adapted with permission from ref.[59]. Copyright 2004 AAAS. (c) Optical routing of a grid-like nanowire connection and (d) PL from the nanowires as the input channel is optically excited. Adapted with permission from ref.[112]. Copyright 2004 National Academy of Sciences. (e) Bright field (left) and second harmonic generation (SHG) (right) images of the optically trapped KNbO3 nanowire. (f) Optical spectra for KNbO3 and Si nanowires. Strong SHG spectrum observed at 532 nm from the KNbO3 nanowire. Adapted with permission from ref.[113]. Copyright 2007 Nature Publishing Group. (g) Photonic nanowire-based single cell endoscopy. Adapted with permission from ref.[114]. Copyright 2011 Nature Publishing Group.

3.2 Metallic nanowires for plasmonic waveguides

While photonic waveguides have been demonstrated using dielectric nanowires, plasmonic waveguides have been limited to use chemically-synthesized Group 11 transition metals (Au, Ag, and Cu) to minimize propagation losses from surface roughness and crystal quality.[111] Among the metals, since Au and Cu have absorption losses in the visible range due to their d-band transitions, Ag nanowire is the most widely studied for plasmonic waveguides, but Ag is chemically less stable

than Au under ambient conditions which can increase propagation loss, mainly due to ohmic loss. From last decades, although Ag nanowire-based plasmonic waveguides have been intensively studied, the measured propagation lengths have been shown significant discrepancies based on their diameter and the measurement conditions.[111,115-117] To elucidate this inconsistency, a chemically-grown Ag nanowire-based SPP modes have been discovered by using a tapered optical fiber tip touching to a suspended Ag nanowire.[115] Two lowest order modes (H_0 and H_1) having different propagation distances and their interference mode are shown in Figures 10a-b. These multi-SPP modes on Ag nanowires have been decoupled and analyzed based on the Ag nanowire diameters and excitation wavelengths by developing a mode interference method. The different behaviors of two SPP modes can be originated from the excitation wavelength, plasmonic waveguide size, and substrates. For applications, the lowest order mode with the highest momentum is ideal for optical imaging which requires high spatial resolution, while the higher order mode is preferred in optical sensing which requires a larger skin depth.

On an Au nanowire, SPPs excitation has been demonstrated by using a scanning tunneling microscopy (STM) tip.[29] Low-energy electrons generated via a STM tip excite gap plasmons, which couple to propagating SPPs under ambient conditions. Figures 10c-d show a micron-long, chemically-grown Au nanowire and a photon emission map. From this work, the simple nanowire-based structure and the required low voltage provide a potential compatibility with current complementary metal oxide semiconductor technology.

For optical elements integration, a structure-dependent SPPs loss such as bending loss has to be also considered. Bending loss in an Ag nanowire has been demonstrated in Figure 10e. In general, the loss increases significantly as the Ag nanowire bending radius increases due to a high refractive index difference.[116] As we discussed earlier, the higher order SPPs modes are not

strongly confined to the Ag nanowire surface and a large fraction of the evanescence fields are scattered at the bending area. In opposite, the lowest order SPPs mode with higher momentum is tightly bound on the surface which results in a lower energy leakage. However, the coupling strength of the lowest mode decreases in the larger diameter of Ag nanowires and thus most of energy leaks through the bending area. Although the bending loss can be minimized in Ag nanowires with small diameter by tight confinement of SPPs modes, it results in a large Ohmic loss. Consequently, for high performance SPPs-based optical elements, a geometry of metal nanowires should be carefully considered to balance both bending and Ohmic losses.

The advantages of the plasmonic nanowire, energy propagation at the metal surface and a stronger evanescent field, provide a higher sensitivity for optical sensing applications. For example, surface enhanced Raman spectroscopy (SERS) can be demonstrated by incorporating localized SPPs to significantly enhance the electromagnetic field, which allows to detect low concentration of molecules. Figure 10f shows an experimental setup to detect Raman modes from a single living cell using a plasmonic nanowire waveguide mounted on a tungsten tip. This approach enables to detect clear Raman modes of biomolecules including proteins and lipids.[118]

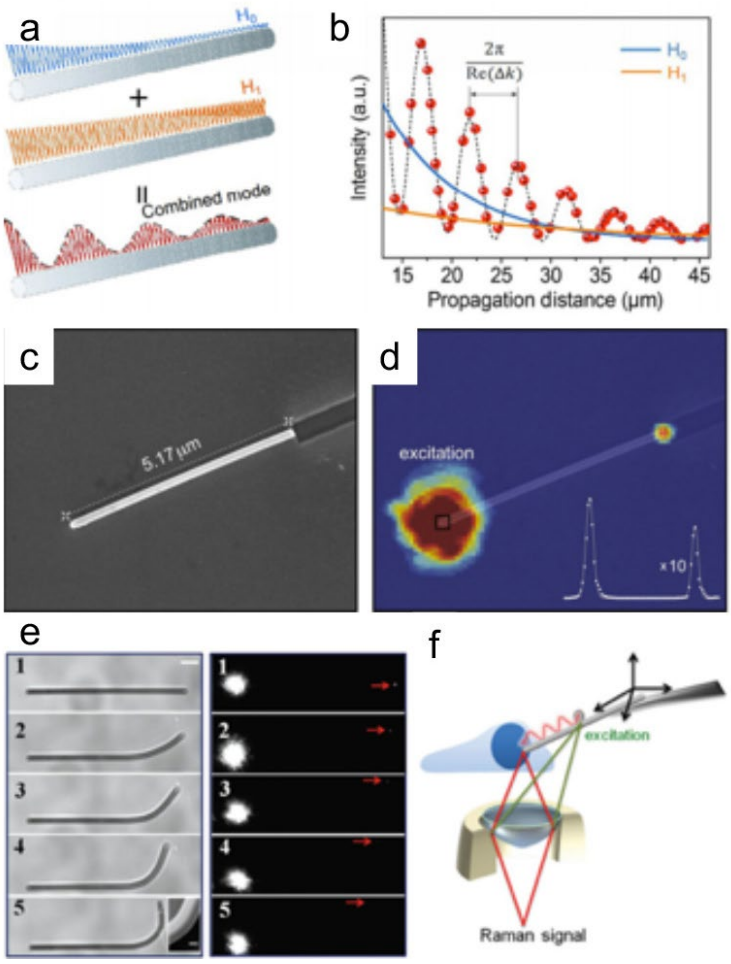

Figure 10. Applications of plasmonic nanowire waveguides. (a) Two lowest order SPP modes in an Ag nanowire. (b) Measured plasmonic emission intensity as a function of propagation distance. Adapted with permission from ref.[115]. Copyright 2017 Springer. (c-d) SEM image of an Au nanowire and overlaid spatial emission profiles. Adapted with permission from ref.[29]. Copyright 2011 American Physical Society. (e) Bright field optical images (left) and corresponding dark field optical images with different bending radii. Adapted with permission from ref.[116]. Copyright 2011 American Chemical Society. (f) Schematic illustration of an Ag nanowire based plasmonic SERS probe. Adapted with permission from ref.[118]. Copyright 2014 John Wiley and Sons.

3.3 Photonic-plasmonic hybrid nanowire waveguides

In the previous sections, we discuss two different waveguides based on photonic or plasmonic nanowires. Although many research progresses have been made, fundamental limitations (i.e., diffraction limit for photonic nanowires and Ohmic lose for plasmonic nanowires) are still remaining to solve for optically integrated circuit miniaturization. To satisfy the requirements for high performance photonic circuit, mainly deep subwavelength mode and low light loss, new hybrid waveguide concepts by combining photonic and plasmonic components have been emerged over the last decade.[111,119-121] For the integration of two different type of optical components, light should be transferred to each other by optical coupling. First demonstration of the hybrid structure is SnO2 (dielectric) – Ag (plasmonic) – SnO2 (dielectric) coupled structure (Figure 11a) for an optical routing circuit.[119] The two SnO2 nanoribbons were connected with an Ag nanowire. While the straight SnO2 nanoribbon was not excited in the absence of the Ag nanowire, a significant optical enhancement was observed when the Ag nanowire is optically bridging two ribbons by launching the SPPs in the Ag nanowire (Figure 11b).[119] However, the large surface roughness and poor crystallinity of the Ag nanowire is still remained as a challenge for practical applications.

Although the dielectric-metallic hybrid structure has not yet fully optimized for the optical routing circuit, it has been successfully demonstrating nanoscale plasmonic lasers. Figure 11c shows a schematic of a hybrid structure, CdS (dielectric nanowire)/MgF2 (dielectric spacer)/Ag (metallic substrate).[120] This structure generates deep subwavelength plasmonic laser at visible frequencies with six-fold enhancement of the spontaneous emission rate. The simulated electric field distribution and directions of a hybrid plasmonic mode are shown in Figure 11d.[120] Subsequently, room-temperature laser has been demonstrated using a single InGaN/GaN core/shell nanorod on an SiO_2 covered with an Ag film (Figures 11e-f).[121] An epitaxially grown

Ag film induce the reduction of mode volume and propagation loss. However, lasing at room temperature with improved temperature stability is still remaining to solve. As one effort, a quantum dot-based hybrid structure has been demonstrated with low lasing threshold and a significant improvement of temperature stability (7 – 125 K).[122] As opposed to the coherent lasing demonstration on a hybrid structure, a single InAsP quantum dot embedded in a vertically-grown InP photonic nanowire waveguide has been used to demonstrate bright single photon emitters. Since single photons emitted from the quantum dot propagate in the InAsP waveguide, a metallic Au layer was deposited on the substrate as a mirror at the nanowire base to reflect downward-emitted photons, which can significantly reduce optical losses.[123]

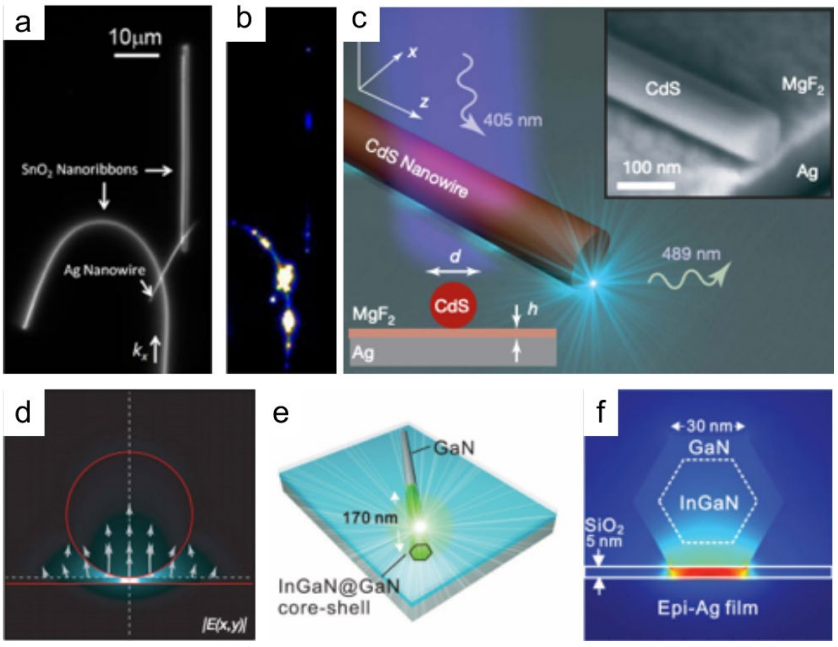

Figure 11. Applications of photonic-plasmonic hybrid nanowire waveguides. (a-b) Optical routing between SnO_2 (dielectric)-Ag (metallic)-SnO_2 (dielectric) hybrid waveguides. Adapted with permission from ref.[119]. Copyright 2008 Nature Publishing Group. (c-d) Plasmonic laser generation and the corresponding electric field distribution from CdS/MgF_2/Ag hybrid structure. Adapted with permission from ref.[120]. Copyright 2009 Nature Publishing Group. (e-f) Schematic and energy density distribution of a single InGaN/GaN core-shell structure on an epitaxially grown Ag film. Adapted with permission from ref.[121]. Copyright 2012 AAAS.

4. Towards All-Photonic Integrated Circuit

In spite of remarkable progresses in nanowire-based photonics in the last decade, enormous challenges remain for alternating current microelectronics industry to photonic integrated circuit. First one is high-quality nanowire synthesis. Although a wide range of nanowires including semiconducting, plasmonic, and dielectric nanowires has been exploited for photonic elements demonstrations, there are still many improvements such as impurities, chemical stability, structure control, etc. For example, atomic-level defects can increase optical loss in photonic and plasmonic waveguides. Emerging halide perovskite-based nanowire is needed to minimize ambient conditions to avoid chemical degradation. Nanowire synthesis in largescale with reliable reproducibility is also critical for practical photonic circuit demonstration. Second, multi-dimensional nanowire assembly technique is still missing. Langmuir-Blodgett assembly has been a promising approach to organize macroscopic numbers of nanowires over substrates. However, it lacks single-nanowire spatial controllability and a compatibility to water-sensitive nanowire compositions. As alternative approaches, optical trapping method has been investigated to manipulate non-metallic nanowires with highly focused laser beams in aqueous chambers.[113] In addition to the physical assembly, each nanowire should be coupled optically to transfer light from emitter to detector through waveguides with minimum optical losses.

Recently, as a prototype, an InGaN/GaN core-shell photonic nanowire with five radial quantum-wells based emitter and detector were integrated on-chip through a SiN waveguide (Figures 12a-b).[124] However, the device performance is still premature (e.g., extremely slow on-off time of ~0.5 s) possibly due to low charge injection efficiency or poor optical couplings of each elements. Another attempt is implemented photonic elements into existing electronic devices.[125] For the efficient conversion from optical to electric signal, metallic nanowire-based plasmonic

waveguides were used. Figure 12c shows an experimental schematic of the propagating SPP modes in an Ag nanowire which coupled to Ge nanowire photodetectors. Here, the ratio of detected charges through the Ge nanowire to the number of SPPs from the Ag-Ge junction is defined as the plasmon-charge conversion efficiency, which is ~0.1 electrons/plasmon. Furthermore, the Ag nanowire plays an additional role as a gate electrode to improve the conversion efficiency up to 50 electrons/plasmon via a plasmonic gating effect.[125] More recently, a plasmonic-silicon nanowire array based integrated circuit has been reported to generate and detect ultra-broadband waveforms in the terahertz range.[126] This system is combined optical-terahertz wave (O/T) and terahertz wave-electronic (T/E) converters with silicon-based photonic devices as illustrated in Figure 12e. A false-color scanning electron microscopy image of an O/T and T/E converters are shown in Figure 12e (upper inset). To form the plasmonic-silicon hybrid structure, a narrow silicon nanowire waveguide was combined with overlays of Au and Ti layer (lower inset, Figure 12e). This approach demonstrates co-integration of terahertz wave transmitters and receivers on the silicon photonic platform, which allows nanowire-based on-chip optoelectronic signal processors.[126]

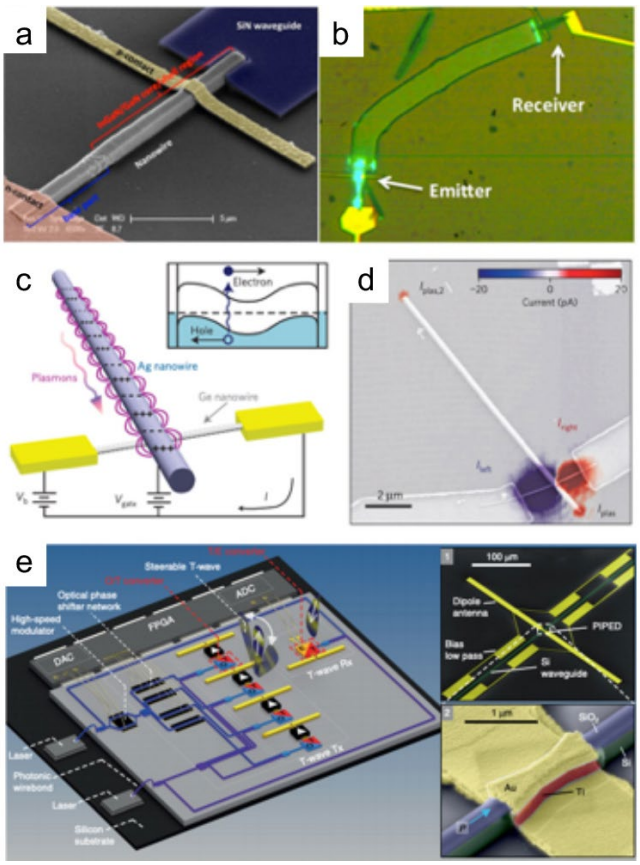

Figure 12. Prototypes of photonic integrated circuit. (a-b) False color SEM and optical microscopy images of a single nanowire-based integrated LED and photodetector. Adapted with permission from ref.[124]. Copyright 2014 American Chemical Society. (c-d) Schematic and SEM images of electrical plasmon detector implemented with a nanowire field-effect transistor. Adapted with permission from ref.[125]. Copyright 2009 Nature Publishing Group. (e) An integrated system for terahertz wave generation and detection includes O/T and T/E converters based on thin plasmonic metal layers coated Si nanowires. Adapted with permission from ref.[126]. Copyright 2018 Nature Publishing Group.

Although the fundamental properties are almost clear from the prototype demonstrations, the applicable photonic circuits are still far behind than microelectronics. Most importantly, electron-photon inter-controllability is the most urgent hurdle to overcome, for example, electrically-driven light generation or efficient electric signal generation from injected photons. Improved device geometries and fabrication are required without significantly degrading the

optical signal propagation. Assuming the electrically-driven photonic device structures are fully optimized, further systematic investigation is required to fully maximize the device performances such as photon-electron conversion efficiency, lifetime, and reproducibility. At the same time, more fundamentally, additional optical components such as optical coupler, splitter, polarizer, and modulator should be considered as well as emitter, detector, and waveguide applications, for all photonic elements-based circuit integration.

5. Conclusion

One-dimensional nanowires are a promising material structure for photonic applications. These nanowires can be categorized into semiconducting, metallic, and dielectric nanowires based on chemical compositions and optical properties, and each exhibit light generation, plasmonic, and photonic waveguides, respectively. Semiconducting nanowire-based light generation covers lasing and light emitting diodes. Particularly, nanowires having well-defined facets show the coherent light generation and their tunable bandgap provides multi-wavelength light emitting properties. However, it is still required to optimize the emitting device structures to demonstrate electrically-driven light controllability. The metallic and dielectric nanowires are utilized for light confinement and propagation as a waveguide. Based on the propagating mechanisms, plasmonic and photonic waveguides are introduced using metallic and dielectric nanowires, respectively. To balance between high optical loss from plasmonic waveguides and diffraction limit of photonic waveguide, both structures can be hybridized to take each advantage. Lastly, all-photonic elements-based integrated circuit as an ultimate goal has been discussed by introducing the current efforts of prototype demonstrations for next-generation photonic devices.

Acknowledgement

L.N.Q, J.K. and P.D.Y acknowledge the U.S. Department of Energy, Office of Science, Office of Basic Energy Sciences, Materials Sciences and Engineering Division, under Contract DE-AC02-05CH11231 within the Physical Chemistry of Inorganic Nanostructures Program (KC3103). J.K. further acknowledges IBS Global Postdoctoral Fellowship (IBS-R026-D1). C.Z.N. thanks Tsinghua University and the 985 University Program for support during the writing of this manuscript.

References

(1) Dasgupta, N. P.; Sun, J.; Liu, C.; Brittman, S.; Andrews, S. C.; Lim, J.; Gao, H.; Yan, R.; Yang, P. 25th anniversary article: semiconductor nanowires–synthesis, characterization, and applications. *Adv. Mater.* **2014,** *26* (14), 2137.

(2) Yang, P. D. The chemistry and physics of semiconductor nanowires. *MRS Bull.* **2005,** *30* (2), 85.

(3) Martensson, T.; Svensson, C. P. T.; Wacaser, B. A.; Larsson, M. W.; Seifert, W.; Deppert, K.; Gustafsson, A.; Wallenberg, L. R.; Samuelson, L. Epitaxial III-V nanowires on silicon. *Nano Lett.* **2004,** *4* (10), 1987.

(4) Gagliano, L.; Belabbes, A.; Albani, M.; Assali, S.; Verheijen, M. A.; Miglio, L.; Bechstedt, F.; Haverkort, J. E.; Bakkers, E. P. Pseudodirect to Direct Compositional Crossover in Wurtzite GaP/InxGa1-xP Core-Shell Nanowires. *Nano Lett.* **2016,** *16* (12), 7930.

(5) Kuykendall, T.; Ulrich, P.; Aloni, S.; Yang, P. Complete composition tunability of InGaN nanowires using a combinatorial approach. *Nat. Mater.* **2007,** *6* (12), 951.

(6) Yang, Z. Y.; Xu, J. Y.; Wang, P.; Zhuang, X. J.; Pan, A. L.; Tong, L. M. On-Nanowire Spatial Band Gap Design for White Light Emission. *Nano Lett.* **2011,** *11* (11), 5085.

(7) Yang, Z. Y.; Wang, D. L.; Meng, C.; Wu, Z. M.; Wang, Y.; Ma, Y. G.; Dai, L.; Liu, X. W.; Hasan, T.; Liu, X.et al. Broadly Defining Lasing Wavelengths in Single Bandgap-Graded Semiconductor Nanowires. *Nano Lett.* **2014,** *14* (6), 3153.

(8) Pan, A. L.; Zhou, W. C.; Leong, E. S. P.; Liu, R. B.; Chin, A. H.; Zou, B. S.; Ning, C. Z. Continuous Alloy-Composition Spatial Grading and Superbroad Wavelength-Tunable Nanowire Lasers on a Single Chip. *Nano Lett* **2009,** *9* (2), 784.

(9) Pan, A.; Liu, R.; Sun, M.; Ning, C. Z. Quaternary alloy semiconductor nanobelts with bandgap spanning the entire visible spectrum. *J. Am. Chem. Soc.* **2009,** *131* (27), 9502.

(10) Pan, A. L.; Liu, R. B.; Sun, M. H.; Ning, C. Z. Spatial Composition Grading of Quaternary ZnCdSSe Alloy Nanowires with Tunable Light Emission between 350 and 710 nm on a Single Substrate. *ACS Nano* **2010,** *4* (2), 671.

(11) Gu, F. X.; Yang, Z. Y.; Yu, H. K.; Xu, J. Y.; Wang, P.; Tong, L. M.; Pan, A. L. Spatial Bandgap Engineering along Single Alloy Nanowires. *J. Am. Chem. Soc.* **2011,** *133* (7), 2037.

(12) Liu, Z. C.; Yin, L. J.; Ning, H.; Yang, Z. Y.; Tong, L. M.; Ning, C. Z. Dynamical Color-Controllable Lasing with Extremely Wide Tuning Range from Red to Green in a Single Alloy Nanowire Using Nanoscale Manipulation. *Nano Lett.* **2013,** *13* (10), 4945.

(13) Zhang, D. D.; Eaton, S. W.; Yu, Y.; Dou, L. T.; Yang, P. D. Solution-Phase Synthesis of Cesium Lead Halide Perovskite Nanowires. *J Am Chem Soc* **2015,** *137* (29), 9230.

(14) Eaton, S. W.; Lai, M. L.; Gibson, N. A.; Wong, A. B.; Dou, L. T.; Ma, J.; Wang, L. W.; Leone, S. R.; Yang, P. D. Lasing in robust cesium lead halide perovskite nanowires. *Proc. Natl. Acad. Sci. U.S.A.* **2016,** *113* (8), 1993.

(15) Dou, L.; Lai, M. L.; Kley, C. S.; Yang, Y. M.; Bischak, C. G.; Zhang, D. D.; Eaton, S. W.; Ginsberg, N. S.; Yang, P. D. Spatially resolved multicolor CsPbX3 nanowire heterojunctions via anion exchange. *Proc. Natl. Acad. Sci. U.S.A.* **2017,** *114* (28), 7216.

(16) Fan, F.; Turkdogan, S.; Liu, Z. C.; Shelhammer, D.; Ning, C. Z. A monolithic white laser. *Nat. Nanotechnol.* **2015,** *10* (9), 796.

(17) Yan, R. X.; Gargas, D.; Yang, P. D. Nanowire photonics. *Nat. Photonics* **2009,** *3* (10), 569.
(18) Whang, D.; Jin, S.; Wu, Y.; Lieber, C. M. Large-scale hierarchical organization of nanowire arrays for integrated nanosystems. *Nano Lett* **2003,** *3* (9), 1255.
(19) Domurath, B. The Light Amplification by Stimulated-Emission of Radiation (Laser) Physics and Protection by Laser for Employers in Medicine .1. *Z Klin Med* **1990,** *45* (5), 453.
(20) Maslov, A. V.; Ning, C. Z. Reflection of guided modes in a semiconductor nanowire laser. *Appl Phys Lett* **2003,** *83* (6), 1237.
(21) Roder, R.; Ronning, C. Review on the dynamics of semiconductor nanowire lasers. *Semicond Sci Tech* **2018,** *33* (3).
(22) Eaton, S. W.; Fu, A.; Wong, A. B.; Ning, C. Z.; Yang, P. D. Semiconductor nanowire lasers. *Nat Rev Mater* **2016,** *1* (6).
(23) Qian, F.; Lieber, C. M. Semiconductor nanowire lasers. *Ieee Leos Ann Mtg* **2007**, 831.
(24) Pauzauskie, P. J.; Sirbuly, D. J.; Yang, P. D. Semiconductor nanowire ring resonator laser. *Phys. Rev. Lett.* **2006,** *96* (14).
(25) Greytak, A. B.; Barrelet, C. J.; Li, Y.; Lieber, C. M. Semiconductor nanowire laser and nanowire waveguide electro-optic modulators. *Appl Phys Lett* **2005,** *87* (15).
(26) Huang, M. H.; Mao, S.; Feick, H.; Yan, H. Q.; Wu, Y. Y.; Kind, H.; Weber, E.; Russo, R.; Yang, P. D. Room-temperature ultraviolet nanowire nanolasers. *Science* **2001,** *292* (5523), 1897.
(27) Huang, M. H.; Mao, S.; Feick, H.; Yan, H.; Wu, Y.; Kind, H.; Weber, E.; Russo, R.; Yang, P. Room-temperature ultraviolet nanowire nanolasers. *Science* **2001,** *292* (5523), 1897.
(28) Gradecak, S.; Qian, F.; Li, Y.; Park, H. G.; Lieber, C. M. GaN nanowire lasers with low lasing thresholds. *Appl Phys Lett* **2005,** *87* (17).
(29) Bharadwaj, P.; Bouhelier, A.; Novotny, L. Electrical excitation of surface plasmons. *Phys Rev Lett* **2011,** *106* (22), 226802.
(30) Johnson, J. C.; Choi, H. J.; Knutsen, K. P.; Schaller, R. D.; Yang, P. D.; Saykally, R. J. Single gallium nitride nanowire lasers. *Nature materials* **2002,** *1* (2), 106.
(31) Gao, H. W.; Fu, A.; Andrews, S. C.; Yang, P. D. Cleaved-coupled nanowire lasers. *P Natl Acad Sci USA* **2013,** *110* (3), 865.
(32) Das, A.; Heo, J.; Jankowski, M.; Guo, W.; Zhang, L.; Deng, H.; Bhattacharya, P. Room Temperature Ultralow Threshold GaN Nanowire Polariton Laser. *Phys. Rev. Lett.* **2011,** *107* (6).
(33) Qian, F.; Li, Y.; Gradecak, S.; Park, H. G.; Dong, Y. J.; Ding, Y.; Wang, Z. L.; Lieber, C. M. Multi-quantum-well nanowire heterostructures for wavelength-controlled lasers. *Nature materials* **2008,** *7* (9), 701.
(34) Agarwal, R.; Barrelet, C. J.; Lieber, C. M. Lasing in single cadmium sulfide nanowire optical cavities. *Nano Lett* **2005,** *5* (5), 917.
(35) Pan, A. L.; Liu, R. B.; Zhang, Q. L.; Wan, Q.; He, P. B.; Zacharias, M.; Zou, B. S. Fabrication and red-color lasing of individual highly uniform single-crystal CdSe nanobelts. *J Phys Chem C* **2007,** *111* (38), 14253.
(36) Xiao, Y.; Meng, C.; Wu, X. Q.; Tong, L. M. Single mode lasing in coupled nanowires. *Appl Phys Lett* **2011,** *99* (2).

(37) Saxena, D.; Mokkapati, S.; Parkinson, P.; Jiang, N.; Gao, Q.; Tan, H. H.; Jagadish, C. Optically pumped room-temperature GaAs nanowire lasers. *Nat Photonics* **2013,** *7* (12), 963.
(38) Chen, R.; Tran, T. T. D.; Ng, K. W.; Ko, W. S.; Chuang, L. C.; Sedgwick, F. G.; Chang-Hasnain, C. Nanolasers grown on silicon. *Nat Photonics* **2011,** *5* (3), 170.
(39) Mayer, B.; Rudolph, D.; Schnell, J.; Morkotter, S.; Winnerl, J.; Treu, J.; Muller, K.; Bracher, G.; Abstreiter, G.; Koblmuller, G.et al. Lasing from individual GaAs-AlGaAs core-shell nanowires up to room temperature. *Nat Commun* **2013,** *4*.
(40) Zapien, J. A.; Jiang, Y.; Meng, X. M.; Chen, W.; Au, F. C. K.; Lifshitz, Y.; Lee, S. T. Room-temperature single nanoribbon lasers. *Appl Phys Lett* **2004,** *84* (7), 1189.
(41) Chin, A. H.; Vaddiraju, S.; Maslov, A. V.; Ning, C. Z.; Sunkara, M. K.; Meyyappan, M. Near-infrared semiconductor subwavelength-wire lasers. *Appl Phys Lett* **2006,** *88* (16).
(42) Gao, Q.; Saxena, D.; Wang, F.; Fu, L.; Mokkapati, S.; Guo, Y. A.; Li, L.; Wong-Leung, J.; Caroff, P.; Tan, H. H.et al. Selective-Area Epitaxy of Pure Wurtzite InP Nanowires: High Quantum Efficiency and Room-Temperature Lasing. *Nano Lett* **2014,** *14* (9), 5206.
(43) Choi, H. J.; Johnson, J. C.; He, R. R.; Lee, S. K.; Kim, F.; Pauzauskie, P.; Goldberger, J.; Saykally, R. J.; Yang, P. D. Self-organized GaN quantum wire UV lasers. *Journal of Physical Chemistry B* **2003,** *107* (34), 8721.
(44) Ning, C. Z.; Dou, L. T.; Yang, P. D. Bandgap engineering in semiconductor alloy nanomaterials with widely tunable compositions. *Nat. Rev. Mat.* **2017,** *2* (12).
(45) Hu, S. Y.; Miller, M. S.; Young, D. B.; Yi, J. C.; Leonard, D.; Gossard, A. C.; Petroff, P. M.; Coldren, L. A.; Dagli, N. Optical Gain Anisotropy in Serpentine Superlattice Nanowire-Array Lasers. *Appl. Phys. Lett.* **1993,** *63* (15), 2015.
(46) Hu, S. Y.; Yi, J. C.; Miller, M. S.; Leonard, D.; Young, D. B.; Gossard, A. C.; Dagli, N.; Petroff, P. M.; Coldren, L. A. Serpentine Superlattice Nanowire-Array Lasers. *IEEE J. Quantum Electron.* **1995,** *31* (8), 1380.
(47) Skold, N.; Karlsson, L. S.; Larsson, M. W.; Pistol, M. E.; Seifert, W.; Tragardh, J.; Samuelson, L. Growth and optical properties of strained GaAs-GaxIn1-xP core-shell nanowires. *Nano Lett.* **2005,** *5* (10), 1943.
(48) Yang, Z.; Wang, D.; Meng, C.; Wu, Z.; Wang, Y.; Ma, Y.; Dai, L.; Liu, X.; Hasan, T.; Liu, X.et al. Broadly defining lasing wavelengths in single bandgap-graded semiconductor nanowires. *Nano Lett.* **2014,** *14* (6), 3153.
(49) Hua, B.; Motohisa, J.; Kobayashi, Y.; Hara, S.; Fukui, T. Single GaAs/GaAsP Coaxial Core-Shell Nanowire Lasers. *Nano Lett.* **2009,** *9* (1), 112.
(50) Chen, R.; Tran, T.-T. D.; Ng, K. W.; Ko, W. S.; Chuang, L. C.; Sedgwick, F. G.; Chang-Hasnain, C. Nanolasers grown on silicon. *Nat. Photonics* **2011,** *5* (3), 170.
(51) Mayer, B.; Rudolph, D.; Schnell, J.; Morkotter, S.; Winnerl, J.; Treu, J.; Muller, K.; Bracher, G.; Abstreiter, G.; Koblmuller, G.et al. Lasing from individual GaAs-AlGaAs core-shell nanowires up to room temperature. *Nat Commun* **2013,** *4*, 2931.
(52) Saxena, D.; Mokkapati, S.; Parkinson, P.; Jiang, N.; Gao, Q.; Tan, H. H.; Jagadish, C. Optically pumped room-temperature GaAs nanowire lasers. *Nat. Photonics* **2013,** *7* (12), 963.

(53) Gao, Q.; Saxena, D.; Wang, F.; Fu, L.; Mokkapati, S.; Guo, Y.; Li, L.; Wong-Leung, J.; Caroff, P.; Tan, H. H.et al. Selective-area epitaxy of pure wurtzite InP nanowires: high quantum efficiency and room-temperature lasing. *Nano Lett.* **2014,** *14* (9), 5206.
(54) Xing, G.; Mathews, N.; Lim, S. S.; Yantara, N.; Liu, X.; Sabba, D.; Grätzel, M.; Mhaisalkar, S.; Sum, T. C. Low-temperature solution-processed wavelength-tunable perovskites for lasing. *Nat. Mater.* **2014,** *13*, 476.
(55) Zhu, H.; Fu, Y.; Meng, F.; Wu, X.; Gong, Z.; Ding, Q.; Gustafsson, M. V.; Trinh, M. T.; Jin, S.; Zhu, X. Y. Lead halide perovskite nanowire lasers with low lasing thresholds and high quality factors. *Nat. Mater.* **2015,** *14* (6), 636.
(56) Fu, Y.; Zhu, H.; Schrader, A. W.; Liang, D.; Ding, Q.; Joshi, P.; Hwang, L.; Zhu, X. Y.; Jin, S. Nanowire Lasers of Formamidinium Lead Halide Perovskites and Their Stabilized Alloys with Improved Stability. *Nano Lett.* **2016,** *16* (2), 1000.
(57) Fu, Y.; Zhu, H.; Stoumpos, C. C.; Ding, Q.; Wang, J.; Kanatzidis, M. G.; Zhu, X.; Jin, S. Broad Wavelength Tunable Robust Lasing from Single-Crystal Nanowires of Cesium Lead Halide Perovskites (CsPbX3, X = Cl, Br, I). *ACS Nano* **2016,** *10* (8), 7963.
(58) Evans, C. C.; Liu, C.; Suntivich, J. TiO2 Nanophotonic Sensors for Efficient Integrated Evanescent Raman Spectroscopy. *Acs Photonics* **2016,** *3* (9), 1662.
(59) Law, M.; Sirbuly, D. J.; Johnson, J. C.; Goldberger, J.; Saykally, R. J.; Yang, P. D. Nanoribbon waveguides for subwavelength photonics integration. *Science* **2004,** *305* (5688), 1269.
(60) Barrelet, C. J.; Wu, Y.; Bell, D. C.; Lieber, C. M. Synthesis of CdS and ZnS nanowires using single-source molecular precursors. *J Am Chem Soc* **2003,** *125* (38), 11498.
(61) Johnson, J. C.; Yan, H. Q.; Schaller, R. D.; Haber, L. H.; Saykally, R. J.; Yang, P. D. Single nanowire lasers. *J. Phys. Chem. B* **2001,** *105* (46), 11387.
(62) Yan, H.; He, R.; Johnson, J.; Law, M.; Saykally, R. J.; Yang, P. Dendritic nanowire ultraviolet laser array. *J. Am. Chem. Soc.* **2003,** *125* (16), 4728.
(63) Hu, Z. F.; Guo, X.; Tong, L. M. Freestanding nanowire ring laser. *Appl. Phys. Lett.* **2013,** *103* (18).
(64) Xiao, Y.; Meng, C.; Wang, P.; Ye, Y.; Yu, H. K.; Wang, S. S.; Gu, F. X.; Dai, L.; Tong, L. M. Single-Nanowire Single-Mode Laser. *Nano Lett* **2011,** *11* (3), 1122.
(65) Li, J. B.; Meng, C.; Liu, Y.; Wu, X. Q.; Lu, Y. Z.; Ye, Y.; Dai, L.; Tong, L. M.; Liu, X.; Yang, Q. Wavelength Tunable CdSe Nanowire Lasers Based on the Absorption-Emission-Absorption Process. *Adv. Mater.* **2013,** *25* (6), 833.
(66) Zhu, H. M.; Fu, Y. P.; Meng, F.; Wu, X. X.; Gong, Z. Z.; Ding, Q.; Gustafsson, M. V.; Trinh, M. T.; Jin, S.; Zhu, X. Y. Lead halide perovskite nanowire lasers with low lasing thresholds and high quality factors. *Nature materials* **2015,** *14* (6), 636.
(67) Liu, P.; He, X. X.; Ren, J. H.; Liao, Q.; Yao, J. N.; Fu, H. B. Organic-Inorganic Hybrid Perovskite Nanowire Laser Arrays. *Acs Nano* **2017,** *11* (6), 5766.
(68) Xing, J.; Liu, X. F.; Zhang, Q.; Ha, S. T.; Yuan, Y. W.; Shen, C.; Sum, T. C.; Xiong, Q. H. Vapor Phase Synthesis of Organometal Halide Perovskite Nanowires for Tunable Room-Temperature Nanolasers. *Nano Lett* **2015,** *15* (7), 4571.
(69) Park, K.; Lee, J. W.; Kim, J. D.; Han, N. S.; Jang, D. M.; Jeong, S.; Park, J.; Song, J. K. Light-Matter Interactions in Cesium Lead Halide Perovskite Nanowire Lasers. *J Phys Chem Lett* **2016,** *7* (18), 3703.

(70) Fu, Y. P.; Zhu, H. M.; Stoumpos, C. C.; Ding, Q.; Wang, J.; Kanatzidis, M. G.; Zhu, X. Y.; Jin, S. Broad Wavelength Tunable Robust Lasing from Single-Crystal Nanowires of Cesium Lead Halide Perovskites (CsPbX3, X = Cl, Br, I). *Acs Nano* **2016,** *10* (8), 7963.
(71) Gu, Z. Y.; Wang, K. Y.; Sun, W. Z.; Li, J. K.; Liu, S.; Song, Q. H.; Xiao, S. M. Two-Photon Pumped CH3NH3PbBr3 Perovskite Microwire Lasers. *Adv Opt Mater* **2016,** *4* (3), 472.
(72) Fu, Y. P.; Zhu, H. M.; Schrader, A. W.; Liang, D.; Ding, Q.; Joshi, P.; Hwang, L.; Zhu, X. Y.; Jin, S. Nanowire Lasers of Formamidinium Lead Halide Perovskites and Their Stabilized Alloys with Improved Stability. *Nano Lett* **2016,** *16* (2), 1000.
(73) Lee, J. W.; Kim, D. H.; Kim, H. S.; Seo, S. W.; Cho, S. M.; Park, N. G. Formamidinium and Cesium Hybridization for Photo- and Moisture-Stable Perovskite Solar Cell. *Adv Energy Mater* **2015,** *5* (20).
(74) Nedelcu, G.; Protesescu, L.; Yakunin, S.; Bodnarchuk, M. I.; Grotevent, M. J.; Kovalenko, M. V. Fast Anion-Exchange in Highly Luminescent Nanocrystals of Cesium Lead Halide Perovskites (CsPbX3, X = Cl, Br, I). *Nano Lett* **2015,** *15* (8), 5635.
(75) Protesescu, L.; Yakunin, S.; Bodnarchuk, M. I.; Krieg, F.; Caputo, R.; Hendon, C. H.; Yang, R. X.; Walsh, A.; Kovalenko, M. V. Nanocrystals of Cesium Lead Halide Perovskites (CsPbX3, X = Cl, Br, and I): Novel Optoelectronic Materials Showing Bright Emission with Wide Color Gamut. *Nano Lett* **2015,** *15* (6), 3692.
(76) Zhang, D. D.; Yang, Y. M.; Bekenstein, Y.; Yu, Y.; Gibson, N. A.; Wong, A. B.; Eaton, S. W.; Kornienko, N.; Kong, Q.; Lai, M. L.et al. Synthesis of Composition Tunable and Highly Luminescent Cesium Lead Halide Nanowires through Anion-Exchange Reactions. *J Am Chem Soc* **2016,** *138* (23), 7236.
(77) Chen, J.; Fu, Y. P.; Samad, L.; Dang, L. N.; Zhao, Y. Z.; Shen, S. H.; Guo, L. J.; Jin, S. Vapor-Phase Epitaxial Growth of Aligned Nanowire Networks of Cesium Lead Halide Perovskites (CsPbX3, X = Cl, Br, I). *Nano Lett* **2017,** *17* (1), 460.
(78) Lu, D.; Zhang, Y.; Lai, M. L.; Lee, A.; Xie, C. L.; Lin, J.; Lei, T.; Lin, Z. N.; Kley, C. S.; Huang, J. M.et al. Giant Light-Emission Enhancement in Lead Halide Perovskites by Surface Oxygen Passivation. *Nano Lett* **2018,** *18* (11), 6967.
(79) Lai, M. L.; Obliger, A.; Lu, D.; Kley, C. S.; Bischak, C. G.; Kong, Q.; Lei, T.; Dou, L. T.; Ginsberg, N. S.; Limmer, D. T.et al. Intrinsic anion diffusivity in lead halide perovskites is facilitated by a soft lattice. *Proc. Natl. Acad. Sci. U.S.A.* **2018,** *115* (47), 11929.
(80) Lu, D.; Zhang, Y.; Lai, M.; Lee, A.; Xie, C.; Lin, J.; Lei, T.; Lin, Z.; Kley, C. S.; Huang, J.et al. Giant Light-Emission Enhancement in Lead Halide Perovskites by Surface Oxygen Passivation. *Nano Lett.* **2018,** *18* (11), 6967.
(81) Konenkamp, R.; Word, R. C.; Schlegel, C. Vertical nanowire light-emitting diode. *Appl. Phys. Lett.* **2004,** *85* (24), 6004.
(82) Qian, F.; Li, Y.; Gradecak, S.; Wang, D. L.; Barrelet, C. J.; Lieber, C. M. Gallium nitride-based nanowire radial heterostructures for nanophotonics. *Nano Lett.* **2004,** *4* (10), 1975.
(83) Gudiksen, M. S.; Lauhon, L. J.; Wang, J.; Smith, D. C.; Lieber, C. M. Growth of nanowire superlattice structures for nanoscale photonics and electronics. *Nature* **2002,** *415* (6872), 617.
(84) Kind, H.; Yan, H. Q.; Messer, B.; Law, M.; Yang, P. D. Nanowire ultraviolet photodetectors and optical switches. *Adv. Mater.* **2002,** *14* (2), 158.

(85) Bao, J. M.; Zimmler, M. A.; Capasso, F.; Wang, X. W.; Ren, Z. F. Broadband ZnO single-nanowire light-emitting diode. *Nano Lett.* **2006,** *6* (8), 1719.
(86) Lupan, O.; Pauporte, T.; Viana, B. Low-Voltage UV-Electroluminescence from ZnO-Nanowire Array/p-GaN Light-Emitting Diodes. *Adv. Mater.* **2010,** *22* (30), 3298.
(87) Lai, E.; Kim, W.; Yang, P. D. Vertical Nanowire Array-Based Light Emitting Diodes. *Nano Research* **2008,** *1* (2), 123.
(88) Zhang, X. M.; Lu, M. Y.; Zhang, Y.; Chen, L. J.; Wang, Z. L. Fabrication of a High-Brightness Blue-Light-Emitting Diode Using a ZnO-Nanowire Array Grown on p-GaN Thin Film. *Adv. Mater.* **2009,** *21* (27), 2767.
(89) Xu, S.; Xu, C.; Liu, Y.; Hu, Y. F.; Yang, R. S.; Yang, Q.; Ryou, J. H.; Kim, H. J.; Lochner, Z.; Choi, S.et al. Ordered Nanowire Array Blue/Near-UV Light Emitting Diodes. *Adv. Mater.* **2010,** *22* (42), 4749.
(90) Huang, Y.; Duan, X. F.; Lieber, C. M. Nanowires for integrated multicolor nanophotonics. *Small* **2005,** *1* (1), 142.
(91) Duan, X. F.; Huang, Y.; Agarwal, R.; Lieber, C. M. Single-nanowire electrically driven lasers. *Nature* **2003,** *421* (6920), 241.
(92) Ding, K.; Yin, L. J.; Hill, M. T.; Liu, Z. C.; van Veldhoven, P. J.; Ning, C. Z. An electrical injection metallic cavity nanolaser with azimuthal polarization. *Appl. Phys. Lett.* **2013,** *102* (4).
(93) Ning, C. Z. Semiconductor nanolasers. *Physica Status Solidi B-Basic Solid State Physics* **2010,** *247* (4), 774.
(94) Ding, K.; Ning, C. Z. Metallic subwavelength-cavity semiconductor nanolasers. *Light-Sci Appl* **2012,** *1*.
(95) Ding, K.; Ning, C. Z. Fabrication challenges of electrical injection metallic cavity semiconductor nanolasers. *Semicond. Sci. Technol.* **2013,** *28* (12).
(96) Ding, K.; Hill, M.; Liu, Z.; Yin, L.; Van Veldhoven, P.; Ning, C. Record performance of electrical injection sub-wavelength metallic-cavity semiconductor lasers at room temperature. *Opt. Express* **2013,** *21* (4), 4728.
(97) Li, D.; Ning, C. Z. Electrical Injection in Longitudinal and Coaxial Heterostructure Nanowires: A Comparative Study through a Three-Dimensional Simulation. *Nano Lett.* **2008,** *8* (12), 4234.
(98) Lim, J. H.; Kang, C. K.; Kim, K. K.; Park, I. K.; Hwang, D. K.; Park, S. J. UV electroluminescence emission from ZnO light-emitting diodes grown by high-temperature radiofrequency sputtering. *Adv. Mater.* **2006,** *18* (20), 2720.
(99) Fang, X.; Li, J. H.; Zhao, D. X.; Shen, D. Z.; Li, B. H.; Wang, X. H. Phosphorus-Doped p-Type ZnO Nanorods and ZnO Nanorod p-n Homojunction LED Fabricated by Hydrothermal Method. *J. Phys. Chem. C* **2009,** *113* (50), 21208.
(100) Chen, M.-T.; Lu, M.-P.; Wu, Y.-J.; Song, J.; Lee, C.-Y.; Lu, M.-Y.; Chang, Y.-C.; Chou, L.-J.; Wang, Z. L.; Chen, L.-J. Near UV LEDs made with in situ doped pn homojunction ZnO nanowire arrays. *Nano Lett.* **2010,** *10* (11), 4387.
(101) Nadarajah, A.; Word, R. C.; Meiss, J.; Konenkamp, R. Flexible inorganic nanowire light-emitting diode. *Nano Lett.* **2008,** *8* (2), 534.

(102) Qian, F.; Gradecak, S.; Li, Y.; Wen, C. Y.; Lieber, C. M. Core/multishell nanowire heterostructures as multicolor, high-efficiency light-emitting diodes. *Nano Lett.* **2005,** *5* (11), 2287.
(103) Duan, X. F.; Huang, Y.; Cui, Y.; Wang, J. F.; Lieber, C. M. Indium phosphide nanowires as building blocks for nanoscale electronic and optoelectronic devices. *Nature* **2001,** *409* (6816), 66.
(104) Minot, E. D.; Kelkensberg, F.; van Kouwen, M.; van Dam, J. A.; Kouwenhoven, L. P.; Zwiller, V.; Borgstrom, M. T.; Wunnicke, O.; Verheijen, M. A.; Bakkers, E. P. A. M. Single quantum dot nanowire LEDs. *Nano Lett.* **2007,** *7* (2), 367.
(105) Wong, A. B.; Lai, M. L.; Eaton, S. W.; Yu, Y.; Lin, E.; Dou, L.; Fu, A.; Yang, P. D. Growth and Anion Exchange Conversion of CH3NH3PbX3 Nanorod Arrays for Light-Emitting Diodes. *Nano Lett.* **2015,** *15* (8), 5519.
(106) Foster, M. A.; Turner, A. C.; Sharping, J. E.; Schmidt, B. S.; Lipson, M.; Gaeta, A. L. Broad-band optical parametric gain on a silicon photonic chip. *Nature* **2006,** *441* (7096), 960.
(107) Jacobsen, R. S.; Andersen, K. N.; Borel, P. I.; Fage-Pedersen, J.; Frandsen, L. H.; Hansen, O.; Kristensen, M.; Lavrinenko, A. V.; Moulin, G.; Ou, H.et al. Strained silicon as a new electro-optic material. *Nature* **2006,** *441* (7090), 199.
(108) Rong, H. S.; Jones, R.; Liu, A. S.; Cohen, O.; Hak, D.; Fang, A.; Paniccia, M. A continuous-wave Raman silicon laser. *Nature* **2005,** *433* (7027), 725.
(109) Leuthold, J.; Koos, C.; Freude, W. Nonlinear silicon photonics. *Nat Photonics* **2010,** *4* (8), 535.
(110) Pauzauskie, P. J.; Yang, P. Nanowire photonics. *Mater Today* **2006,** *9* (10), 36.
(111) Kim, S.; Yan, R. Recent developments in photonic, plasmonic and hybrid nanowire waveguides. *J Mater Chem C* **2018,** *6* (44), 11795.
(112) Sirbuly, D. J.; Law, M.; Pauzauskie, P.; Yan, H.; Maslov, A. V.; Knutsen, K.; Ning, C. Z.; Saykally, R. J.; Yang, P. Optical routing and sensing with nanowire assemblies. *Proc Natl Acad Sci U S A* **2005,** *102* (22), 7800.
(113) Nakayama, Y.; Pauzauskie, P. J.; Radenovic, A.; Onorato, R. M.; Saykally, R. J.; Liphardt, J.; Yang, P. Tunable nanowire nonlinear optical probe. *Nature* **2007,** *447* (7148), 1098.
(114) Yan, R. X.; Park, J. H.; Choi, Y.; Heo, C. J.; Yang, S. M.; Lee, L. P.; Yang, P. D. Nanowire-based single-cell endoscopy. *Nat Nanotechnol* **2012,** *7* (3), 191.
(115) Kim, S.; Bailey, S.; Liu, M.; Yan, R. X. Decoupling co-existing surface plasmon polariton (SPP) modes in a nanowire plasmonic waveguide for quantitative mode analysis. *Nano Res* **2017,** *10* (7), 2395.
(116) Wang, W.; Yang, Q.; Fan, F.; Xu, H.; Wang, Z. L. Light propagation in curved silver nanowire plasmonic waveguides. *Nano Lett* **2011,** *11* (4), 1603.
(117) Wild, B.; Cao, L. N.; Sun, Y. G.; Khanal, B. P.; Zubarev, E. R.; Gray, S. K.; Scherer, N. F.; Pelton, M. Propagation Lengths and Group Velocities of Plasmons in Chemically Synthesized Gold and Silver Nanowires. *Acs Nano* **2012,** *6* (1), 472.
(118) Lu, G.; De Keersmaecker, H.; Su, L.; Kenens, B.; Rocha, S.; Fron, E.; Chen, C.; Van Dorpe, P.; Mizuno, H.; Hofkens, J.et al. Live-cell SERS endoscopy using plasmonic nanowire waveguides. *Advanced materials* **2014,** *26* (30), 5124.
(119) Yan, R.; Pausauskie, P.; Huang, J.; Yang, P. Direct photonic-plasmonic coupling and routing in single nanowires. *Proc Natl Acad Sci U S A* **2009,** *106* (50), 21045.

(120) Oulton, R. F.; Sorger, V. J.; Zentgraf, T.; Ma, R. M.; Gladden, C.; Dai, L.; Bartal, G.; Zhang, X. Plasmon lasers at deep subwavelength scale. *Nature* **2009,** *461* (7264), 629.
(121) Lu, Y. J.; Kim, J.; Chen, H. Y.; Wu, C. H.; Dabidian, N.; Sanders, C. E.; Wang, C. Y.; Lu, M. Y.; Li, B. H.; Qiu, X. G.et al. Plasmonic Nanolaser Using Epitaxially Grown Silver Film. *Science* **2012,** *337* (6093), 450.
(122) Ho, J. F.; Tatebayashi, J.; Sergent, S.; Fong, C. F.; Ota, Y.; Iwamoto, S.; Arakawa, Y. A Nanowire-Based Plasmonic Quantum Dot Laser. *Nano Lett* **2016,** *16* (4), 2845.
(123) Reimer, M. E.; Bulgarini, G.; Akopian, N.; Hocevar, M.; Bavinck, M. B.; Verheijen, M. A.; Bakkers, E. P. A. M.; Kouwenhoven, L. P.; Zwiller, V. Bright single-photon sources in bottom-up tailored nanowires. *Nat Commun* **2012,** *3*.
(124) Tchernycheva, M.; Messanvi, A.; Bugallo, A. D.; Jacopin, G.; Lavenus, P.; Rigutti, L.; Zhang, H.; Halioua, Y.; Julien, F. H.; Eymery, J.et al. Integrated Photonic Platform Based on InGaN/GaN Nanowire Emitters and Detectors. *Nano Lett* **2014,** *14* (6), 3515.
(125) Falk, A. L.; Koppens, F. H. L.; Yu, C. L.; Kang, K.; Snapp, N. D.; Akimov, A. V.; Jo, M. H.; Lukin, M. D.; Park, H. Near-field electrical detection of optical plasmons and single-plasmon sources. *Nat Phys* **2009,** *5* (7), 475.
(126) Harter, T.; Muehlbrandt, S.; Ummethale, S.; Schmid, A.; Neiien, S.; Hahn, L.; Freude, W.; Koos, C. Silicon-plasmonic integrated circuits for terahertz signal generation and coherent detection. *Nat Photonics* **2018,** *12* (10), 625.